Article

Sustainable Slope Stability Analysis: A Critical Study on Methods

Ancuța Rotaru [1,*] , Florin Bejan [1] and Dalia Almohamad [2,3]

1 Department of Transportation Infrastructure and Foundations, Faculty of Civil Engineering and Building Services, "Gheorghe Asachi" Technical University of Iași, 1 Prof. Dr. Doc. Dimitrie Mangeron St., 700050 Iași, Romania; florin.bejan@academic.tuiasi.ro

2 University of Orléans, University of Tours, INSA-CVL, Lamé, EA 7494, 8 Rue Léonard de Vinci, F-45072 Orléans, France; dalia.almohamad@anteagroup.fr

3 Antea Group, ZAC du Moulin, 803 Bd Duhamel du Monceau, 45160 Olivet, France

* Correspondence: ancuta.rotaru@tuiasi.ro

Abstract: When studying the stability of a slope, the first issue that needs to be clarified is the slip surface, which determines the minimum safety factor. The slopes investigated here are homogenous with three distinct gradients (1:1.5; 1:1; 2:1), two defined heights (H-3 m; H-8 m), and four different soil characteristics (S1—clayey silt, S2—sandy clayey silt, S3—sandy silty clay, S4—clay). The purpose of this paper is to develop a new methodology capable of estimating the safety factor and the shape and centre of the critical slip surface, delivering an improved estimate of slope probability of failure, which can represent a significant component in a more precise risk assessment. This paper compares distinct methods used in the slope stability analysis, examining their hypotheses and effects on the estimated safety factor and the centre and shape of the critical slip surface. The study compares the limit equilibrium results with those determined by the shear strength reduction method using an approach based on the upper-bound limit analysis to compare the predictions extracted from these methods with those from the finite element method (FEM) analysis. The finite element method discretizes the soil mass into finite elements. Hence, it establishes a kinematically admissible velocity field searching for the failure mechanism of the slope. Results for FEM show the influence of the slope geometry and the mesh size and density on the safety factor. In the study, plots of the regression curves of five different critical slip surface shapes, including a circular slip surface (benchmark), show that the shape of the failure surface depends on the shape and material of the slope. Furthermore, they show that the critical slip surface layout can approach a logarithmic spiral, damped sinusoid, parabola, etc.; the slip surface is not always circular. The analysis reveals that none of the approaches can consider all uncertainties concerning the factor of safety and the interpretations of critical slip surfaces.

Keywords: slope stability; finite element method; upper-bound analysis; factor of safety; slip surface; optimization

1. Introduction

1.1. Information on Slope Stability Analysis

Natural and artificial slopes can become unstable [1]. Slope stability indicates the condition of slopes that either withstand or undergo movement [2]. Slope stability analysis is a static or dynamic, analytical [3] or numerical method for assessing slope stability and understanding the causes of a slope failure or the factors that trigger a slope movement. Stability analysis answers a problem demanding force and/or moment equilibrium. The ratio between the shear strength and the shear stress expressed as a safety factor defines the slope stability.

The input data for performing a slope stability analysis are determined by: (1) The elevation of the ground on a section perpendicular to the slope. (2) Drilling to identify the stratigraphy

and obtain undisturbed soil samples. (3) Laboratory shear tests of undisturbed samples/each layer. (4) Piezometers inserted in the slope for pore-water pressure measurement.

The slip/failure surface position is revealed once the slope has already failed. Otherwise, the location and shape of the most critical slip surface are unknown [4]. The shape of the undetermined surface is assumed while determining the location. If the shape of the slip surface is either a circular arc (the slope is not homogeneous) or partly circular and partly linear, a grid of centres is selected, with the radius varying at each centre and covering all possible conditions [1]. The shape of the slip surface of layered soil can be shallow, elongated, deep with sharp breaks, or convex.

1.2. Historical Context, Understanding Primary Methods

The idea of discretizing a potential sliding mass into vertical slices was born in the early 20th century. At the beginning and until about 50 years ago, the stability of a slope was mainly analysed by limit equilibrium methods (LEM) based on force and moment equilibrium, while realistic analyses of the slope deformation were not possible. Since then, various approaches have developed as versions of the vertical slice method [5,6]. Alternatively, the horizontal slice method (HSM) routine served for layered soils evaluation and internal stability analyses of reinforced walls [7].

With the development and adaptation of the finite-element methods (FEM) based on the widespread availability of powerful computers, numerical modelling for analysing the stability of earth structures, which is the oldest type of numerical analysis in geoengineering, recently became a popular tool [1].

The limit equilibrium methods most often used for practical problems are (Table 1): (1) methods only for circular slip surfaces, such as (a) the ordinary or Swedish method of slices (Fellenius 1927, 1936), which satisfies the moment equilibrium but does not satisfy horizontal or vertical force equilibrium [5], and (b) Bishop's modified method (Bishop 1955), which satisfies moment equilibrium and vertical force equilibrium but does not satisfy horizontal force equilibrium under both drained and undrained loading conditions [8]; (2) methods for any shape of slip surface, such as (a) Janbu's generalized procedure of slices (Janbu 1968), which satisfies all conditions of equilibrium and allows a variety of numerical problems [9], (b) Morgenstern and Price's method (Morgenstern and Price 1965), which satisfies all conditions of equilibrium and allows varied side force orientations [10], and (c) Spencer's method (Spencer 1967), which satisfies all conditions of equilibrium and assumes side force to be parallel [11]. The iterative procedures underlying methods (2b) and (2c) lead to mathematically more rigorous formulations.

Table 1. Summary of assumptions of LE methods used in the paper.

Method	Circular	Non-Circ.	$\Sigma M = 0$	$\Sigma F = 0$
Ordinary (also known as Swedish, Fellenius)	✓	-	✓	-
Bishop simplified	✓	-	✓	vertical only
Jambu corrected	✓	✓	✓	✓
Morgenstern–Price	✓	✓	✓	✓
Spencer	✓	✓	✓	✓

The limit equilibrium methods used in the paper are as follows:

a. The Swedish circle approach (Ordinary or Fellenius method, 1936) applies to homogeneous soils, stratified soils, fully or partially submerged soils, non-uniform soils, and cases where seepage and pore pressure exist within the soil slope. Fellenius is used to analyse the stability of a slope assuming a circular failure surface. Shear strength along the slip surface contributes by the frictional component, which depends on normal stress. Normal stress changes horizontally at any point on the slip surface. Therefore, the analysis divides the wedge into many vertical slices. The distance between the centroid of the potential moving wedge and the centre of rotation "O" is calculated by dividing the algebraic sum of the weight moment for each slice about centre "O" by

the wedge weight. The safety factor is generated from the momentum equilibrium equation concerning the centre of the potential slip surface (O). Investigations are repeated on different slip surfaces to define the factor of safety.

$$FoS = \frac{\sum_i [c_i \cdot l_i + (N_i - u_i \cdot l_i) tan\phi_i]}{\sum_i (W_i \cdot sin\alpha_i)} \tag{1}$$

where: u_i—the pore-water pressure, c_i, ϕ_i—the effective shear strength parameters, W_i—strip weight, N_i—the normal force at the bottom of the strip, α_i—the inclination of the bottom of the strip, and l_i—the length of the base of the strip.

b. Bishop's simplified method (1955) considers the normal interslice forces but ignores the interslice shear forces. That satisfies the overall equilibrium of moments but not the general equilibrium of horizontal forces, assuming a circular slip surface. The value of the factor of safety is determined by successive iterations.

The methods that consider side forces between slices (e.g., the Janbu method) submit themselves to numerical instability problems under certain conditions [12], and the solution may fail to converge, or the calculated values may be unreasonable [13]. The method using the sums of the forces for all slices makes the hand-calculation of the factor of safety a repetitive and laborious process [14].

The last three methods develop some particularities. Janbu's (1954), Morgenstern and Price's (1965, 1967), and Spencer's (1964) methods are rigorous, because they satisfy all three equations of equilibrium—the balance of horizontal and vertical forces and the balance of moments. The position and direction of interslice forces constitute the distinction between methods.

Janbu's and Spencer's techniques of slope stability analysis use the leapfrog algorithm method (velocity Verlet method) for integrating differential equations of the form $\ddot{x} = d^2x/dt^2 = A(x)$ or equivalently of the form $\dot{v} = dv/dt = A(x)$, $\dot{x} = dx/dt = v$ [13].

c. For a minimal-width slice, the assumption of Janbu's method is that the vertical component of the interslice forces depends on the numerical approximation of the differential equation of the moment equilibrium [15]. The method considers normal interslice forces but ignores interslice shear forces. It satisfies the overall horizontal force equilibrium, not the general moment equilibrium.

d. In the Spencer method (1967), the interslice forces are parallel, and the normal force (N) acts on the centre of the base of each slice [16]. Spencer has developed two equations for the factor of safety; the first one of moment equilibrium and the other one of horizontal force equilibrium. This method adopts a constant relationship between the interslice forces (shear and normal forces). By iterative procedures, the interslice shear alters to a normal ratio until the two safety factors are equal. Finding a shear-normal portion equalizing the two safety factors means that the balance between moment and force is met [17].

e. Morgenstern and Price calculus is similar to Spencer's method but allows various specified interslice force functions.

In the limit equilibrium methods, the soil mass slides along an assumed slip surface without considering deformations or strains [1].

The limit equilibrium methods use the Mohr–Coulomb failure criterion to determine the shear strength along the slip surface. Failure occurs when the shear stress is mobilized along a critical slip surface (CSS). Factor of safety (FoS) is the ratio of the available shear strength to the mobilized shear strength [18]. The available shear strength depends on the soil type and the effective normal stress. Mobilized shear strength depends on external forces acting on the soil mass, such as pore-water pressure, slope cracks, swelling, slickenside formation, clay rock deterioration, creep under permanent load, leaching, strain softening, weathering, and cyclic loading. The sliding mass is divided into slices, the shear and normal inter-slice forces are determined, and force and/or moment equilibrium equations satisfy the static equilibrium conditions [12].

Apart from the fact that statically admissible stress is not guaranteed, the limit equilibrium methods eliminate the need for soil plastic flow rules (constitutive relation). At failure, the soil is expected to be a rigid perfectly plastic medium showing a correspondent flow rule, so that the breakdown techniques adopted by the LEM are commonly dynamically unacceptable. Theoretically, the finite element method, which relies on the stress–strain relationships, provides a comprehensive answer to the slope stability problem.

Modern limit equilibrium software based on these techniques solves problems with complex stratigraphy, uncommon pore-water pressure conditions, any shape of the slip surface, various linear and nonlinear shear strength models, concentrated loads, and structural reinforcement.

The advantage of limit analysis is that it uses the associated plastic flow, neglected by the limit equilibrium methods. Based on the plasticity upper-bound theory, the kinematic approach of limit analysis can identify the shape of the slip surface that depends on the plastic criterion of the soil mass and its plastic flow [19–21]. The finite element method (FEM), constructed by Zienkiewicz (1975), uses the shear strength reduction procedure (SSR), also known as the strength reduction factor (SRF), to estimate the safety factor by an elastic–plastic finite element analysis by decreasing the soil strength variables gradually until failure. For simple geometrically definable surfaces (Lighthall, 1979; Prater, 1979) such as sinusoidal slip surfaces, the slip surfaces are distinguished by some patterns. The analysis of each slip surface is completed, and the critical one is chosen [22].

Advantages of the FEM over LEM include the following: (1) There are no initial assumptions associated with the shape or position of the failure surface. (2) There are no assumptions regarding slice side forces. (3) FEM predicts progressive failure up to shear failure. (4) FEM outcomes provide information on predictable deformations.

The experience gained over the last 50 years provides the advantages and limitations of the finite-element method in practical engineering problems [12]. Studies involving other methods may improve the understanding of slope stability problems.

Apart from FEM, some other numerical methods have been recently developed [19,23]: the continuum modelling approach available for the analysis of soil slopes of massive intact rocks, discontinuous modelling for rock slopes controlled by discontinuity behaviour, the perturbation method using the Taylor series expansion of random functions for the mean values [15,24], or the mesh-free Lagrangian method, which is more advantageous when large deformations occur, e.g., the post-failure behaviour of slope, without mesh distortion [25]. Unlike these methods, the semi-analytic modelling technique [26], which allows the modelling of multi-body regions such as the FEM while concurrently sustaining high fidelity and efficiency of analytical solutions, also applies in slope stability analysis.

1.3. Objectives of the Current Research

The present paper determines the factor of safety and coordinates of the centre of the slip surface for five limit equilibrium methods (Fellenius, Bishop simplified, Janbu corrected, Spencer, and Morgenstern–Price) to be compared with the results of the finite element method.

In a comparative study of slope stability analysis, this paper examines the hypotheses of various methods for slope stability analysis and their effects on the estimated FoS. The paper analyses at length two sets of methods used for slope stability: (1) methods based on limit equilibrium (LEM) and (2) an approach based on upper-bound limit analysis, comparing the predictions extracted from these methods to those of FEM analysis performed with PLAXIS® software [27]. This study compares the limit equilibrium results with those determined by the shear strength reduction method. In particular, the slip surface assumes a circular shape in the case of the limit equilibrium method and a logarithmic spiral in the upper-bound limit analysis. However, in this paper, some limitations of those shapes in comparison to the other shapes of slip surfaces such as damped sinusoid (damped sine wave) and parabola are presented. Some case studies have identified the position of the slipping centre, sampling it according to the initial hypothesis of each method.

The examples of slope stability presented in the paper occur in homogenous slopes with various material properties.

2. Materials and Methods

The paper studies the keystone of slope-stability-analysing techniques and the methodology for identifying the centre and shape of the slip surface.

2.1. Limit Equilibrium Methods

When studying the stability of a slope, the first issue that needs to be clarified is that of the slip surface, also known as the critical slip surface in the deterministic method (LEM), which determines the minimum safety factor [28].

The analysis of this surface could have two distinct aspects regarding the method of determination of the FoS:

1. Determination of the geometry of the sliding surface through various hypotheses. The current paper analyses the cylindrical-circular shape (Petterson [29–31] and Fellenius [5,32]) and the logarithmic spiral shape (Rendulic, 1935 [33]).
2. Determining the coordinates of the centre of the slip surface.

Each potential slope failure surface, $Y_f(x)$, has a different factor of safety that can be evaluated by the safety function, $F[Y_f(x)]$. The factor of safety can be found by searching for the critical slope failure surface, $Yc(x)$, associated with the lowest factor of safety.

$$FoS = \min_{Y_f(x)}\{F[Y_f(x)]\} = F[Y_C(x)] \tag{2}$$

The conventional limit equilibrium analysis of slopes involves two steps: (1) Development of response rules between the potential slip surfaces and the factor of safety (FoS). (2) Finding the smallest FoS on all possible slip surfaces. The region representing this minimum value is the critical slip surface [34]. Finding a critical slip surface involves finding the minimum factor of safety, so it makes sense to use an optimization method.

The limit equilibrium is a static indeterminate analysis that shares some typical features and limitations, presuming that the factor of safety is constant along the slip surface, rendering a slope stability problem determinate. This formulation satisfies statics by assuming that forces in the soil mass are such that it stays stationary. The sums of moments, horizontal forces, and vertical forces equal zero (i.e., the factor of safety must reduce the soil strength until the potential sliding mass is a point of limiting equilibrium).

The following assumptions were made: (1) there is a plane stress state, and stresses perpendicular to the section of the soil mass are zero; (2) shear strength parameters c and φ are known; (3) pore-water pressure can be estimated from the known water level and seepage conditions.

All limit equilibrium methods consider the soil mass above the potential slip surface divided into strips (the planes between strips are always vertical). Figure 1a,b shows the forces acting on each strip for the Fellenius method [5].
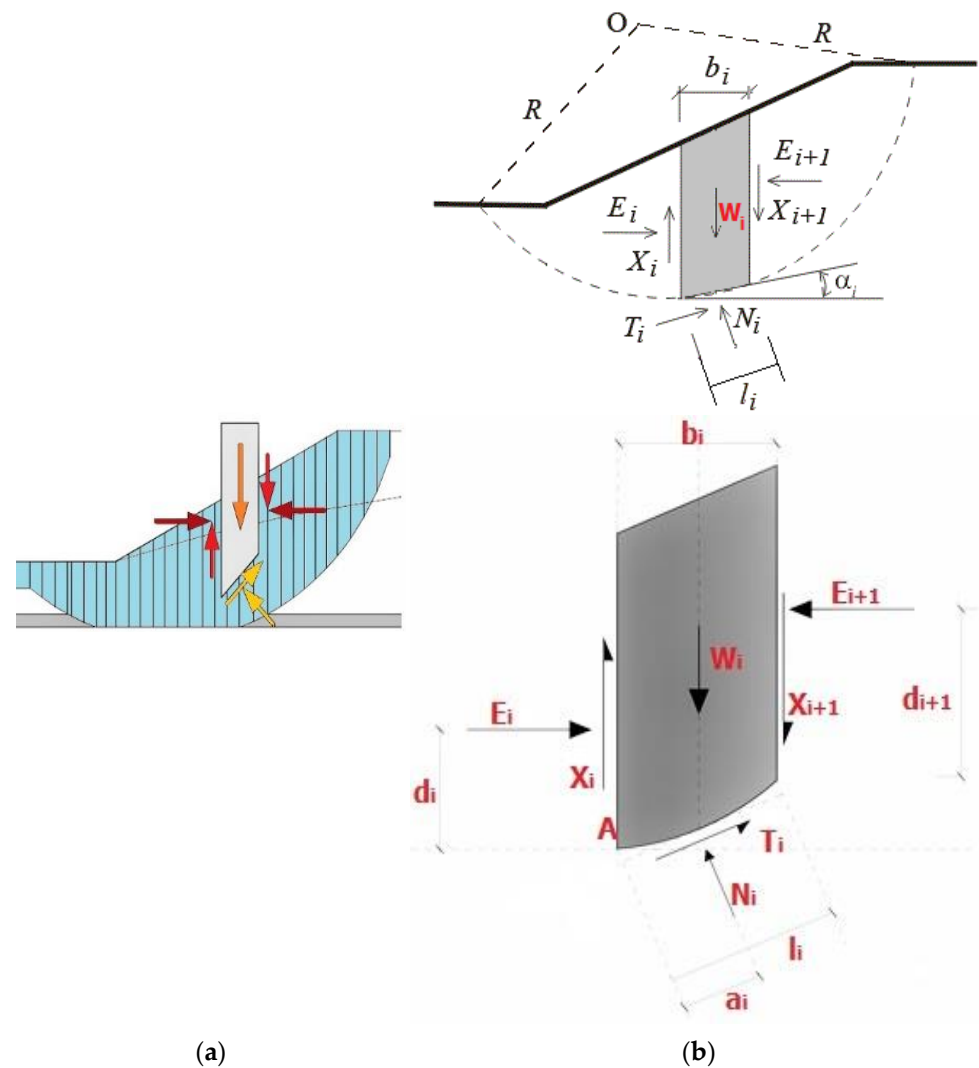
Figure 1. General slope stability problem for the Fellenius method: (**a**) geometry of the problem, (**b**) convention of vector orientations for equilibrium state analysis.

All methods use an identical definition of the factor of safety (FoS).

If the FoS is large enough, the slope is considered stable (safe). If FoS is 1.0 or less, the slope is not safe. The main assumption of the safety factor in limit equilibrium is that it is the same at all points along the slip surface [35].

There are some significant assumptions of the limit equilibrium method of slices regarding the factor of safety: (1) Factor of safety appears as the factor by which the soil strength must lower so that the potential sliding mass is a point of limiting equilibrium. This means that the sum of moments, as well as the sum of forces, must be zero. (2) The factor of safety is constant along the slip surface. (3) Each slice has the same factor of safety.

2.2. The Upper-Bound Limit Method

Chen (1975), Michalowski (1995) [20], and Donald and Chen (1997) elaborated limit analysis methods based on rigid-body plasticity theory to lower the influence of presumptions made in limit equilibrium methods (LEM) on the factor of safety. These methods, giving an upper-bound solution to the value of the safety factor, rely on the upper-bound theorem of limit analysis and are referred to as upper-bound methods [36].

When a given particular structure is under the action of a set of external loads, the upper-bound theorem (UBT) states that structural collapse occurs if the system permits a

compatible displacement field, for which the work of the external loads equals that of the internal stresses [37].

The finite element upper-bound method is a combination of the upper-bound method and the finite element method. The upper-bound theorem considers compatibility conditions and material properties (which govern the work of internal stress) but disregards equilibrium conditions [37]. In the upper-bound limit analysis, the principle of the plastic flow fully defines the shape of the slip surface. Since the soil on a slip surface is assumed to flow plastically, the plastic flow rule and the principle of maximum plastic work constrain the trajectory of any point on that surface. When applying the upper-bound theory to slope stability problems, it is assumed that a slip surface divides the slope into a plastic failure zone during failure. The stress state at any point is on or within the yield plane, and the displacement at any point in the elastic zone is virtually negligible. Shear failure is dominant only within the plastic region along the slip surface. The finite element method is mainly used to discretize the soil mass into finite elements, constructing a kinematically acceptable failure mechanism that can express external and internal work rates [21]. Accordingly, the soil above the slip surface performs a rigid-body rotation with respect to the centre of the slip surface when the sliding occurs. Upper-bound limit analysis provides a suitable solution for homogeneous slope stability. The upper-bound formulation arises from the virtual working velocity equation in the form of factor of safety and the limit load of the slope acting on the top of the slope [38]. The problem of finding the optimal upper-bound solution is transformed to solve a programming problem using the Excel Solver. The FoS solution is calculated and then compared with the outcomes of Slope2 Rocscience.

The slope failure mechanism provides a continuous stress and velocity field except along a slip surface, where the plastic velocity in the elastic zone changes rapidly to zero through a very narrow shear band (Figure 2).
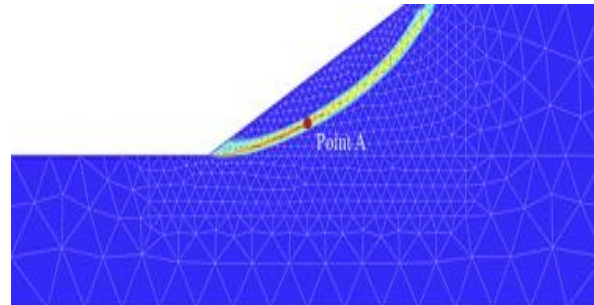
Figure 2. Thin shear band.

Various optimization methods support the determination of the critical failure mode that determines the minimum safety factor. A slip surface divides by some nodal points with coordinates given by (i = 1, 2, . . . , m), as Figure 3 shows. Evaluating the slope stability becomes a numerical problem of finding a set of variables that yield the minimum FoS with the associated slip surface connected by the nodal points.

Figure 3. Nodal points.

The pink points in Figure 3 are included in the schematic diagram of the steps for the identification of the critical slip surface for a 2D homogeneous slope: (a) clustering of the nodal displacements, (b) obtaining the boundary points of the clustering sets, (c) extracting the scatters near the critical slip surface identified in 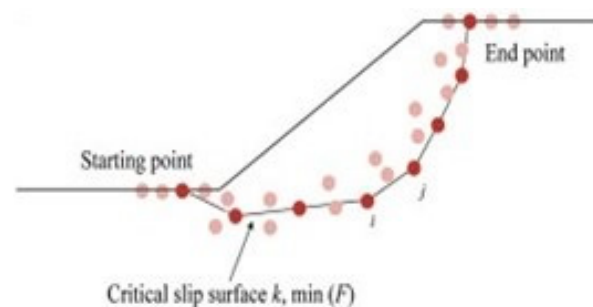FEM, and (d) fitting the critical slip surface in 2D. The pink points are the scatters near the separation surface (the critical slip surface), i.e., step c.

The technique for finding the minimum safety factor is similar to the one that the conventional methods apply. Of all possible slip surfaces, the one with the highest probability of slip has the minimum value of the FoS, being the critical slip surface.

On the other hand, with LEM, it is necessary to identify the shape of the critical slip surface (circular or non-circular) before starting the search procedure or analysing both variants. With FEM, this is an automated procedure of searching the critical limit load and associated upper-bound analysis [39]. This is considered a real benefit over LEM, which uses either a grid method or a random slip surface generator procedure. In this paper, the objective function, which determines the minimum value of the safety factor and constrains equations, derived from a plastic energy–work balance equation of the movement of any point on the slip surface, the Mohr–Coulomb failure (yield) criterion, and boundary conditions.

For a homogenous soil, the potential failure surface is fully identified once the centre of the slip surface is known. For a given slope and potential sliding surface, it is possible to calculate the ratio between resistance moments due to friction and cohesion and active moment (due to gravity). The minimum of these ratios represents the FoS of the slope.

The objective function with constraints leads to a standard nonlinear programming problem solved by a sequential algorithm [40]. Seeking the optimal upper-bound solution transforms into solving a problem within numerous kinematically admissible velocity fields. This issue occurs due to using the point algorithm implemented in the Excel Solver. However, applying the upper-bound theorem to slope stability provides uncertain solutions, i.e., upper-bound solutions or approximate solutions, leading to a very narrow spacing around the true (unknown) FoS and the corresponding slip surface [37].

2.3. Methodology for the Centre and Slipping Surface Identification in FEM Analysis

Usually, when numerical methods supported by geotechnical software apply, the shear strength reduction (SSR) technique (Matsui and San, 1992) for homogeneous and non-homogeneous slope stability problems employed by researchers (e.g., Griffiths and Lane, 1999) can be used to obtain the FoS [22].

Following this strategy, the strength parameters of the constitutive model used to describe the soil behaviour are simultaneously diminished by the same factor up to the failure of the slope. The slope failure is revealed by some numerical indicators; more frequently, the norm of the displacement vector is chosen as such and compared to some limited big numbers. The factor to which the strength parameters are reduced at the moment of failure also represents the FoS. Since the analysis is performed with no hypothesis about the slip surface or/and slipping centre, to obtain information about them, the following four-step procedure establishes displacement boundaries of slope stability problem:

1. Based on the slope stability problem results, identify a set of points on the slip surface. These points can be identified as the ones separating the slip block (large displacement) from the unmovable soil masses (Figure 4).

Figure 4. Illustration of the point pick-up procedure on the slip surface.

2. Using the coordinates of the set points in 1, find the best fit using the least-squares method and the slip surface equations. Construct a system of two equations: the general equation of the second-order surface and a spiral logarithmic one using a non-linear least-squares procedure.
3. Using the coefficients of surfaces identified in 2, find the nature of the slip surface and its parameters.
4. For the slip surface identified in step 3, estimate the centre of the slip surface.

After applying the least-squares method, the slip centre in step 4 is the point that fits best the condition of rigid-body rotation of the slip block.

3. Results

3.1. Case Studies for the Comparative Study

This paper proposes a calculus for the safety factor and the slip centre for three slopes with particular geometry (Figure 5) and four types of homogeneous soils with specific properties (Table 1) using, on the one hand, various limit equilibrium methods and the upper-bound limit method and, on the other hand, numerical calculations using FEM software. The selected cohesive soils provide varied strength characteristics ranging from almost non-plastic clayey sands to cohesive clays. The cohesion parameter for the cohesionless sand is considered to be as small as near zero to avoid numerical errors [16]. In all cases, there is no external load other than the gravitational force, i.e., body force.

Figure 5. The geometry of slopes (slope models).

Motivation for choosing the four types of soils: The four types of soils are clayey silt, sandy-clayey silt, sandy-silty clay, and clay, as given in Table 2. These types of soils are considered to model different types of soil shear strengths. Table 2 summarises the geotechnical parameters of various soil types. The slip surface of slopes for homogeneous soils can approach a circular cylinder.

Table 2. Geotechnical characteristics of soil.

Type of Soil	γ [kN/m^3]	c' [kPA]	ϕ' [°]
S1⁻clayey silt ($I_P = 12$, $I_C = 0.50$, $e = 0.90$)	18.0	10	18
S2⁻sandy $-$ clayey silt ($I_P = 14$, $I_C = 0.70$, $e = 0.80$)	19.0	15	20
S3⁻sandy $-$ silty clay ($I_P = 16$, $I_C = 0.90$, $e = 0.60$)	19.5	20	24
S4⁻clay ($I_P = 28$, $I_C = 0.80$, $e = 0.55$)	20.0	40	20

Motivation for choosing the three slope angles (gradients): To reveal that, when Varying the slope angle gradually and keeping the height of the slope and the soil parameters constant, the factor of safety increases as the slope angle decreases. The decrease in slope increases the factor of safety almost linearly. There is a strong and opposite relation between slope angle and factor of safety for the four types of soils considered.

Motivation for choosing the two heights (8 m and 3 m, respectively): Results presented in the paper show that the FoS (stability, implicitly) is not independent of the slope height, even in the case of homogeneous slopes. The factor of safety increases as the slope height decreases, as the pair of Tables 3–8 show for the same type of soil and gradient. Results are similar for all the four types of soils investigated and using any method. This indicates a strong relationship between the slope height and the factor of safety.

Additionally, at a lower height, i.e., 3 m height, the failure mode in clays (S4) tends to be base slide for all three gradients, while at 8 m height, the failure mode tends to be toe slide. On sandy soils, the failure mode tends to be toe slide for either 3 m height or 8 m.

The reason why the study presents the stability results at 3 m height derives from the paper carried out by [41], which indicates a lower rate of decrease in the factor of safety for slopes higher than 3 m. For slope heights less than 3 m, the factor of safety increases at a higher rate.

Slope height and slope angle can be optimized to maximize the slope factor of safety. The above tables show that the influence of decreasing slope height and angle simultaneously can also be studied.

For the limit equilibrium method (LEM), the Slide2 Rocscience Program performed the analysis, while the PLAXIS software performed the FEM analysis.

The Slide2 Rocscience Program simplifies the process of finding the safety factor and the critical slip surface on the strength of limit equilibrium methods. The software enables the study of the uncertainties regarding the slope geometry and properties of various soils, the potential failure surfaces, and the use of accurate static methods. It allows for narrowing the range of acceptable solutions and assesses the errors involved in slice methods [8]. The LE methods used in this paper using the Slide2 Rocscience Program are the Fellenius/Petterson method, Bishop method, Janbu method, Morgenstern–Price method, and Spencer method, considering circular slip surfaces. The geometric model was nested into the Slide2 Rocscience Program software, assigning the soil properties for the specified interface [42,43]. In the analysis stage, a circular slip surface was in use. The limit equilibrium method of slices required iterative techniques to solve the nonlinear factor of safety equations and find the coordinates of the slip surface. In Slide2 Rocscience Program, the Grid Search Method was used for locating the Global Minimum safety factor for circular slip surfaces (Figure 6a–e). The slip centre grid specifies the number of grid intervals in the X (80) and Y (100) directions, creating a regular grid of slip centres. Each centre in the

slip centre grid represents the centre of rotation of a series of slip circles. Slide2 uses Slope Limits and Radius Increment to generate the circle's radii at each point.
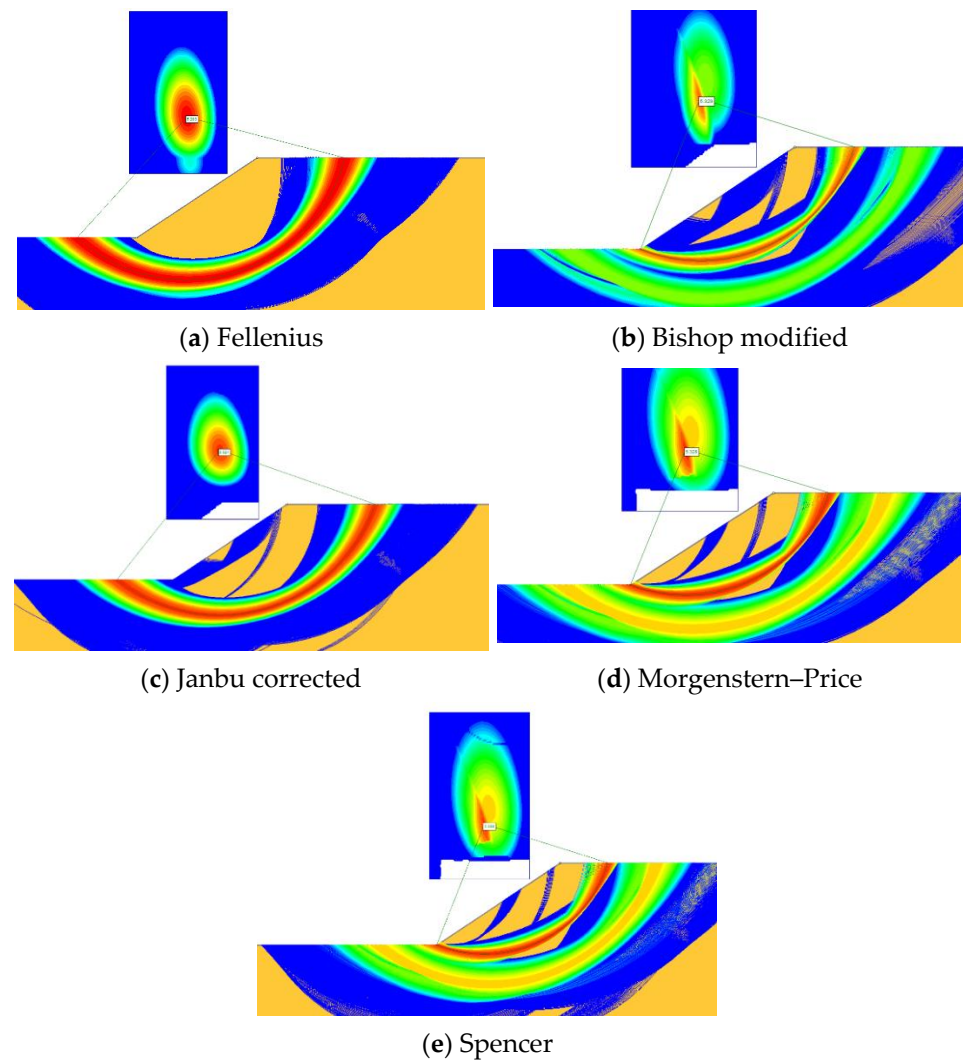

(**a**) Fellenius

(**b**) Bishop modified

(**c**) Janbu corrected

(**d**) Morgenstern–Price

(**e**) Spencer

Figure 6. (**a**–**e**). The circular slip surface for the minimum factor of safety achieved through an optimization algorithm of the Slide2 Rocscience Program for a slope with the geometry 1:1.5, H = 3 m, S4, using five distinct limit methods.

The numerical analysis used PLAXIS (2D), which is a FEM-based software. The slope divides into small elements, and a stress–strain relationship defines each case. The mesh refinement and the number of elements strongly affect the computed FoS.

The selection of the numerical model imposes large enough horizontal and vertical dimensions to not impact the results of the slope stability analysis. In the example illustrated in Figure 7, the lateral dimensions are large, and the model maintains a similar principle regarding the depth to ensure that there is no boundary perturbation. The study considers 50 × 30 m dimensions for the model, foreseeing a slight decrease in the FoS.
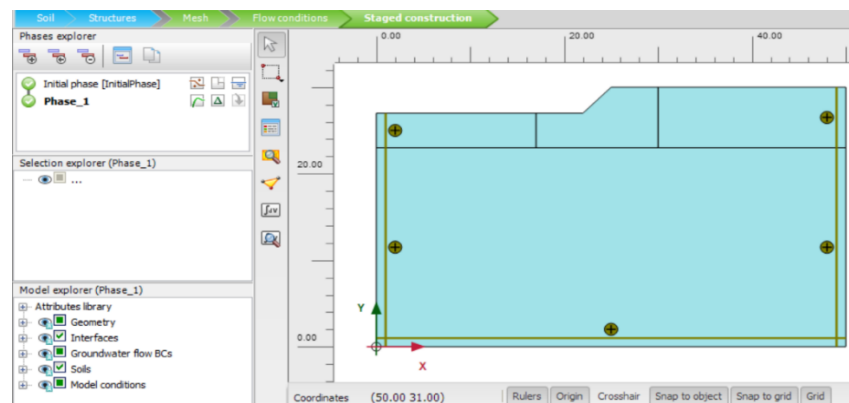
Figure 7. Construction of the model for the slope 1:1, H = 3 m, S1.

All cases analysed operate with plane strains and 15-node triangular elements.

To limit the number of elements, although four polygons were constructed, only the central one had a particularly dense mesh around the slip surface (Figure 8), ten times thicker than the other three polygons, which had moderately dense meshes. The purpose of using a fine mesh is to achieve good accuracy concerning the picked-up points according to the procedure specified in Section 2.3.
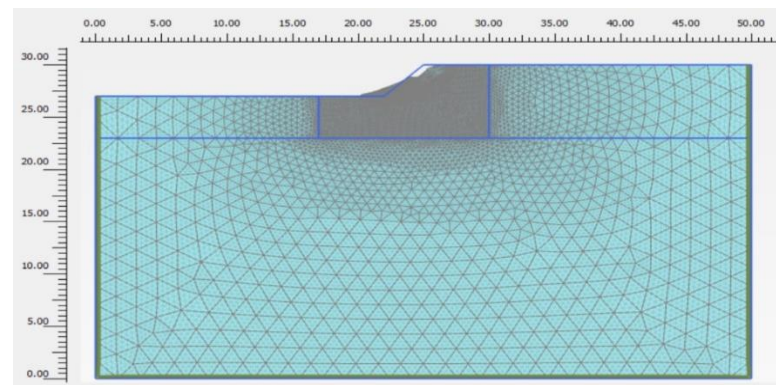

Figure 8. Mesh construction: plane strain and 15-node triangular elements with a fine mesh around the slip surface for the slope 1:1, H = 3 m, S1.

A very dense mesh around the sloping area is an important matter. The finer the mesh, the closer the results will be to each other. However, if the "classical" mesh is maintained, FoS will not decrease dramatically. The analyses used the Mohr–Coulomb failure criterion and a perfect plastic flow with no plastic dilatancy.

3.2. Results

In most of the cases examined, the predicted failure surface passes through the toe of the slope and does not extend below this point. However, in the cases of the 1:1.5, H = 3 m, S2 slope and 1:1, H = 8 m, S1 slope, a base failure occurs, i.e., the failure surface passes below the toe.

The mesh refinement and the number of picked-up elements strongly affect the computed FoS. Furthermore, the adaptive mesh refinement influences the error margin between the upper and lower bounds.

For the cases where the safety factor is greater than 1, the slope yields through the phi-c reduction procedure. In this case, there is no difference between the diagram for total deformation (Phase 1) and that for incremental deformation (Initial Phase) (Figures Figures 9–11 and 12a–h).
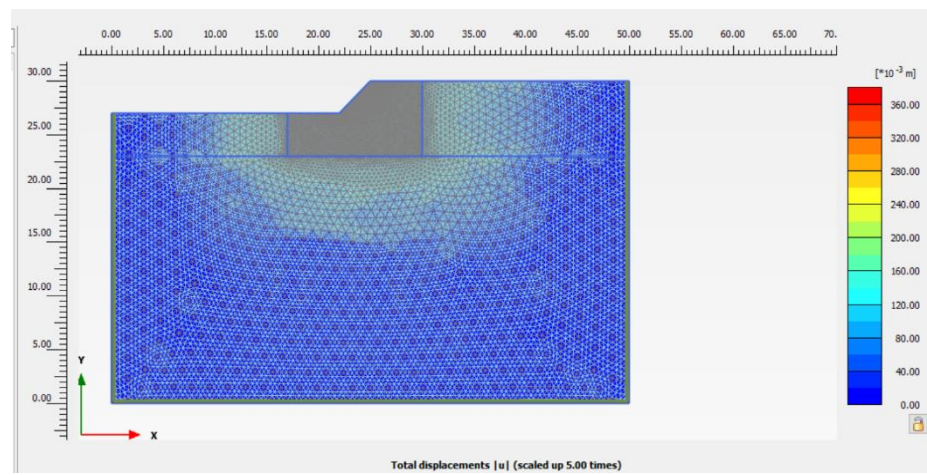
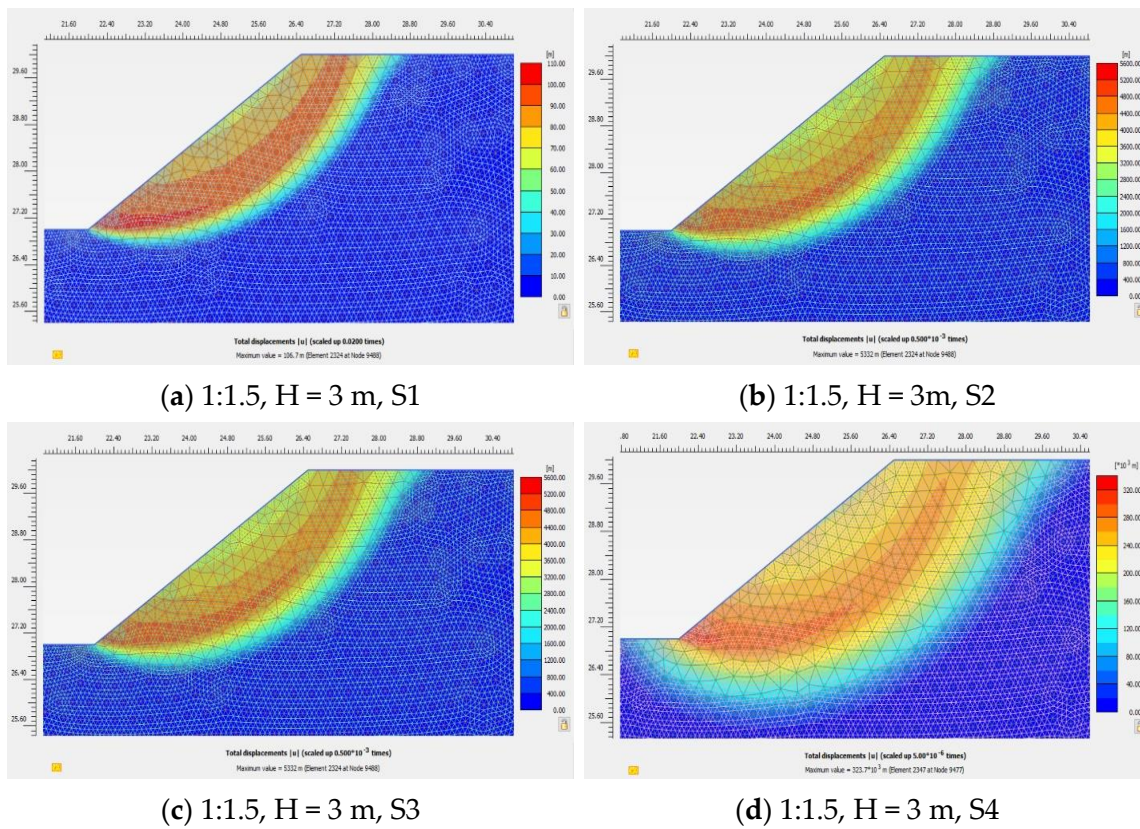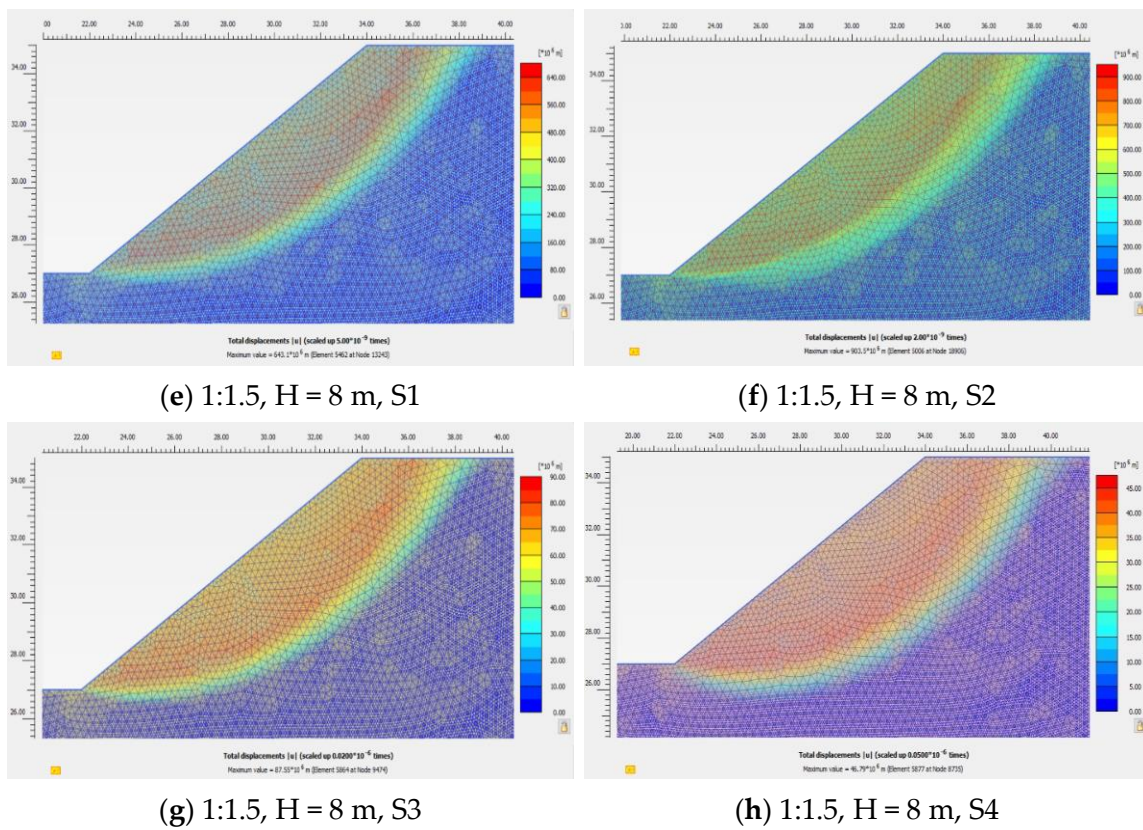**Figure 9.** Total displacements for the slope 1:1, H = 3 m, S1.

(**a**) 1:1.5, H = 3 m, S1

(**b**) 1:1.5, H = 3m, S2

(**c**) 1:1.5, H = 3 m, S3

(**d**) 1:1.5, H = 3 m, S4

Figure 10. *Cont*.

(**e**) 1:1.5, H = 8 m, S1

(**f**) 1:1.5, H = 8 m, S2

(**g**) 1:1.5, H = 8 m, S3

(**h**) 1:1.5, H = 8 m, S4

Figure 10. (**a**–**h**) Soil mass areas prone to move and the slip surfaces for the slope 1:1.5 (8 cases).

(**a**) 1:1, H = 3 m, S1

(**b**) 1:1, H = 3 m, S2

(**c**) 1:1, H = 3 m, S3

(**d**) 1:1, H = 3 m, S4

Figure 11. *Cont.*

(**e**) 1:1, H = 8 m, S1

(**f**) 1:1, H = 8 m, S2

(**g**) 1:1, H = 8 m, S3

(**h**) 1:1, H = 8 m, S4
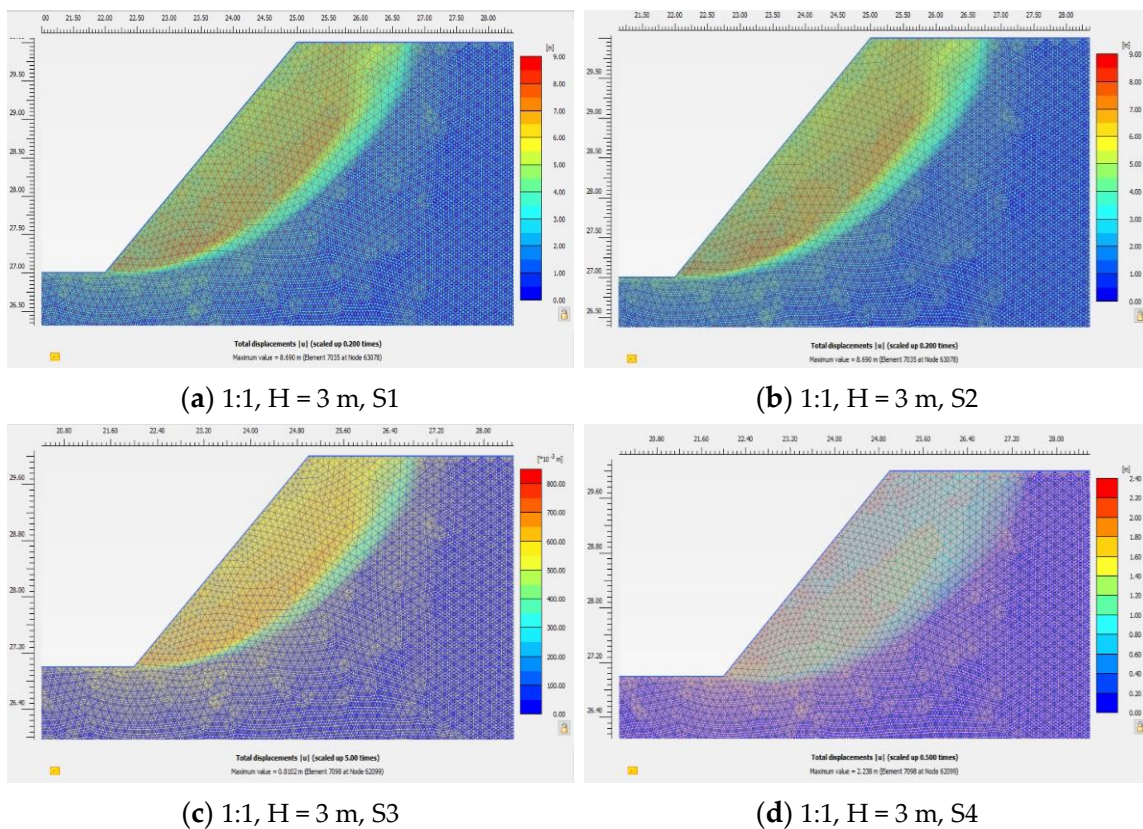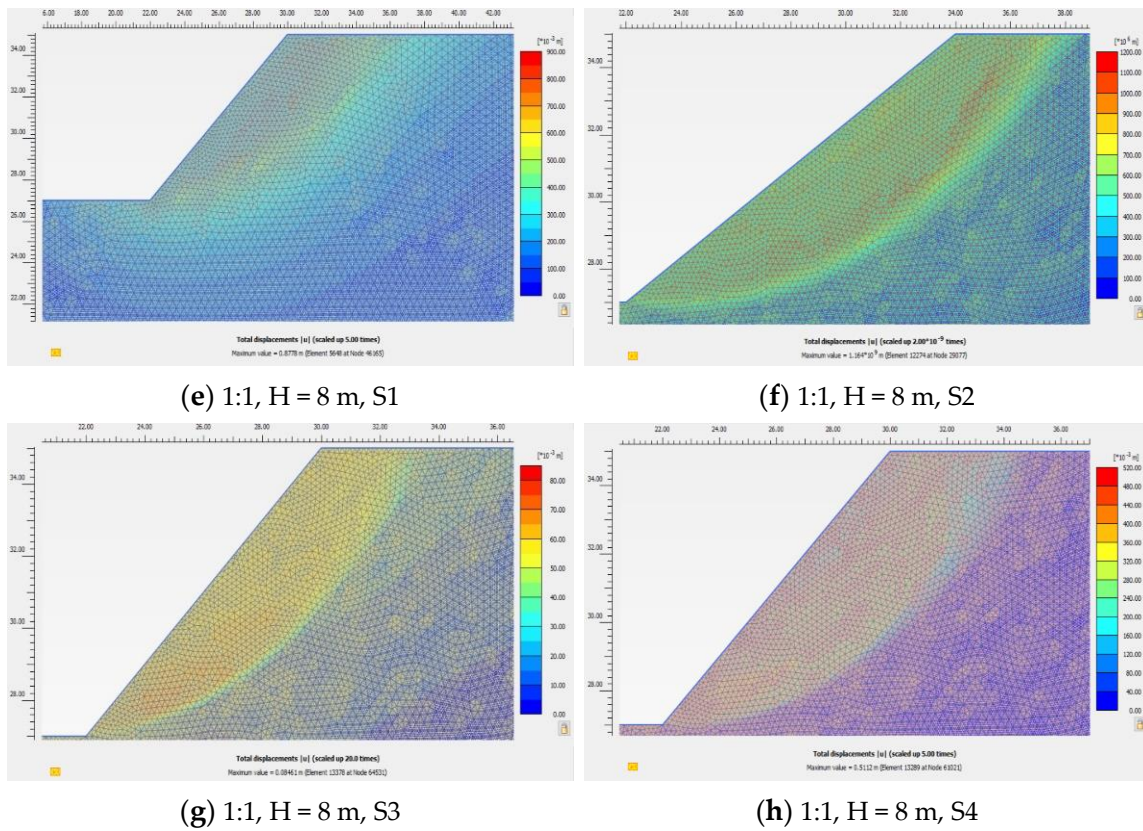
Figure 11. (**a**–**h**) Soil mass areas prone to move and the slip surfaces for the slope 1:1 (8 cases).

(**a**) 2:1, H = 3 m, S1

(**b**) 2:1, H = 3 m, S2

(**c**) 2:1, H = 3 m, S3

(**d**) 2:1, H = 3 m, S4

Figure 12. *Cont*.

(**e**) 2:1, H = 8 m, S1

(**f**) 2:1, H = 8 m, S2

(**g**) 2:1, H = 8 m, S3

(**h**) 2:1, H = 8 m, S4

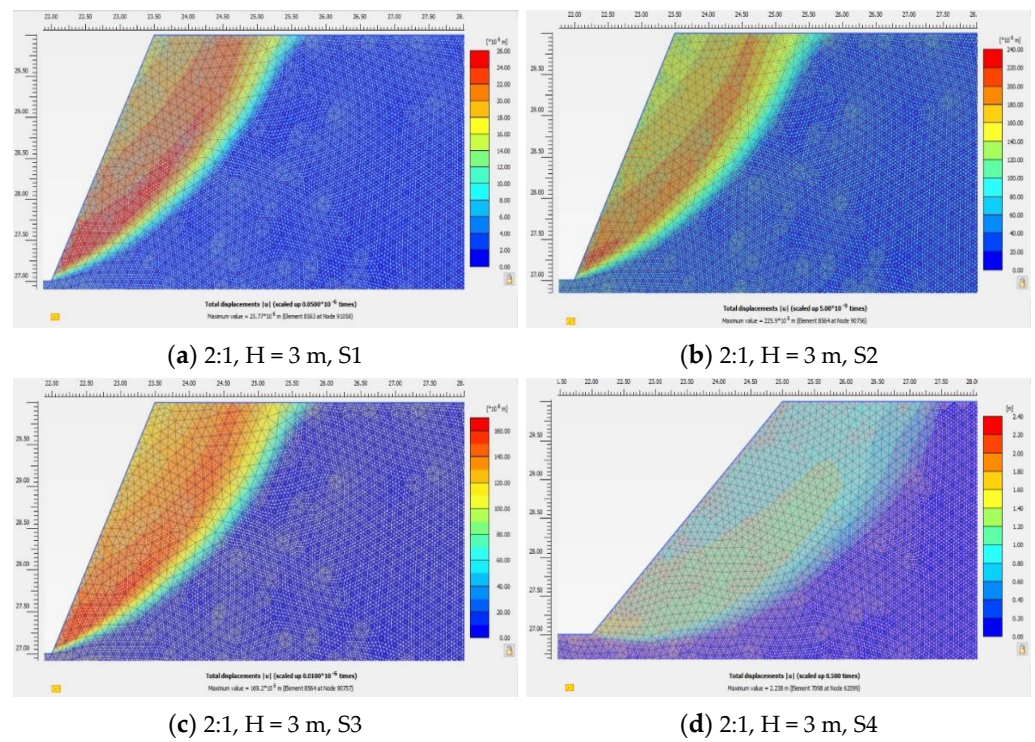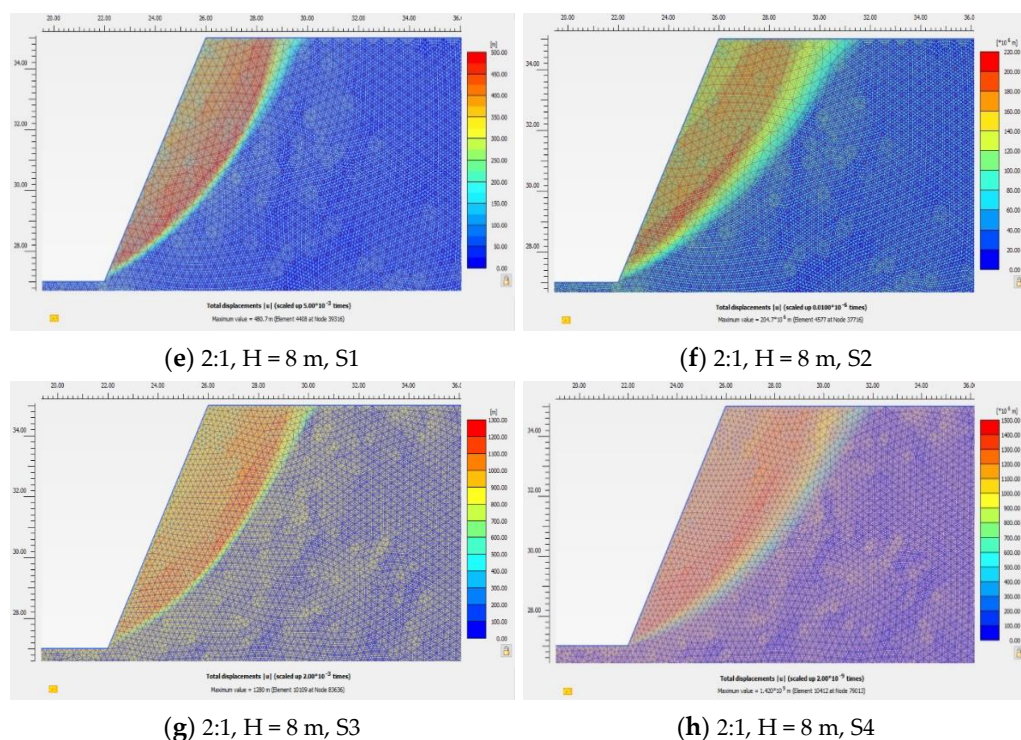**Figure 12.** (**a**–**h**) Soil mass areas prone to move and the slip surfaces for the slope 2:1 (8 cases).

If the stability factor is less than 1.00 (Slope 1:1, H = 8.00 m, S1; Slope 2:1, H = 8.00 m, S1; Slope 2:1, H = 8.00 m, S2), the slope yields from gravitational loading (Initial Phase).

Figure 13 shows the plastic points for the Slope 1:1, H = 8.00 m, S1, and Figure 14 shows the result for the total deformation, a representation that cannot be useful for determining the slip surface.
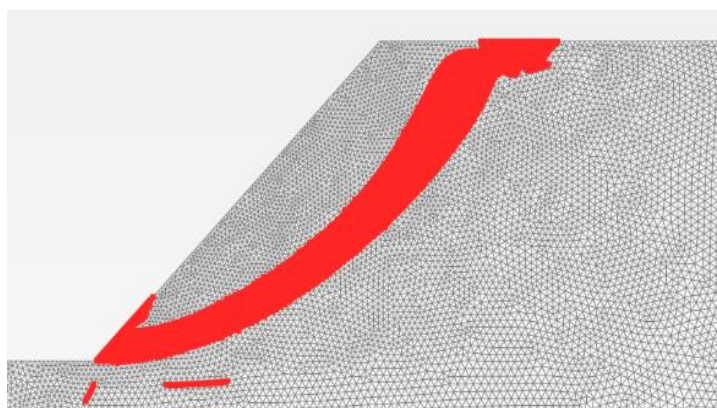

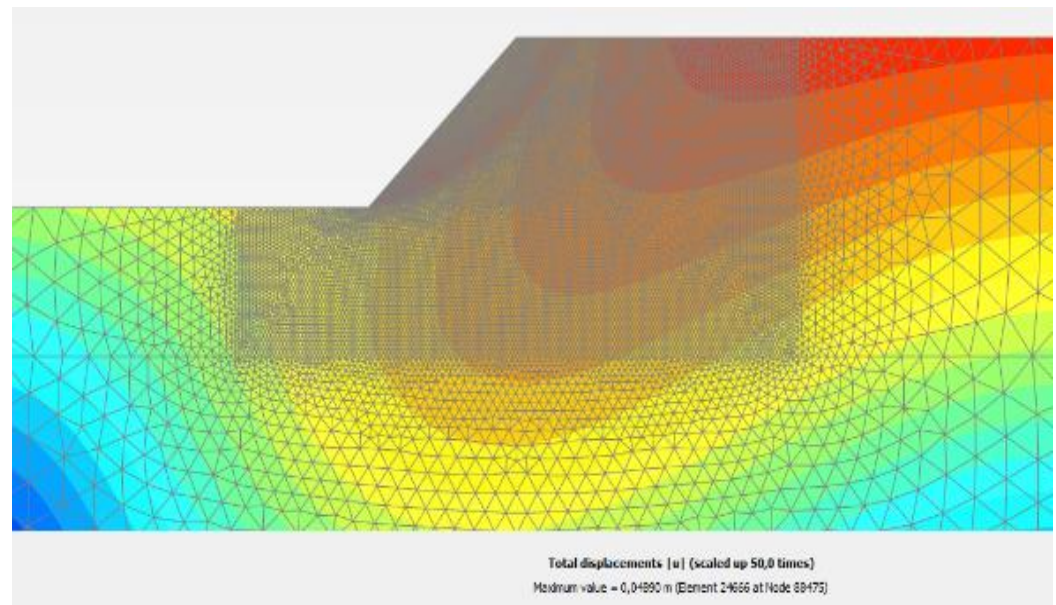**Figure 13.** Plastic deformation 1:1, H = 8 m, S1.

Figure 14. Total deformation 1:1, H = 8 m, S1 (Phase 1).

In these cases, the problem reduces to extracting from the diagram of incremental deformations that follow the slip surface (yielding surface) those points on the band of "0" (Figure 15).
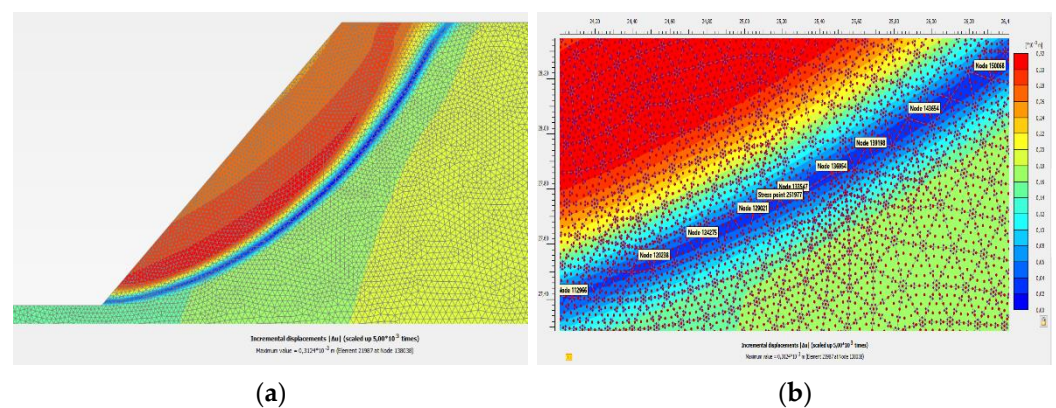

(**a**)

(**b**)

Figure 15. Diagram of incremental deformations. (**a**) Slip surface; (**b**) Picked-up points on "0" band.

Since the block slips, the boundaries slip. Therefore, the slip surface consists of the sum points that (1) develop very slight displacements compared to the slip block and (2) are near the points with large displacements.

Picking up some of the points with a displacement very close to zero from all those points along the line separating the slip block from the unmoving soil mass, reading their coordinates, and then writing their coordinates to an Excel file required creating a table consisting of enough points supposed to define the slip surface. However, the coordinates of the centre of the circular slip surface (if it is a circle) were not yet obtained. The programme found (Xc, Yc).

Three points are enough to define a circle if all three are eligible for selection, and the surface is a circle. However, since there were errors in picking up the points (because of both the mesh and the subjective interpretation of the so-called "close to zero points"), an adjustment of the perfect circle was needed, which was achieved by applying the least-squares method.

The objective consisted of adjusting the parameters of the chosen model function to best fit data sets. The data set used in this study consists of "n" picked-up points for

each case (data pairs) (x_i, y_i), $i = 1, \ldots, n$, where "x" is an independent variable, and "y" is a dependent variable, with the values found by observation. The fitting of the model distribution to a data point was measured by its residual, which is defined as the difference between the observed value of the dependent variable and the fitting value predicted by the model used on the result of each equation. The least-squares method approximated the solutions, finding the optimal parameter values by minimizing the sum of squared residuals.

Tables 3–8 and Figures 16–21 present the safety factors resulting from five LE methods (Slope2 Rocscience) [3] and FEM (PLAXIS 2D). All regarded LE methods consider the slip surface to be circular. The comparative results between FEM, also considering circular slip surfaces (the benchmark), and LEM found that, commonly, the FoS are similar.

Table 3. Results for Slope 1:1.5, H = 3.0 m, S1–S4.

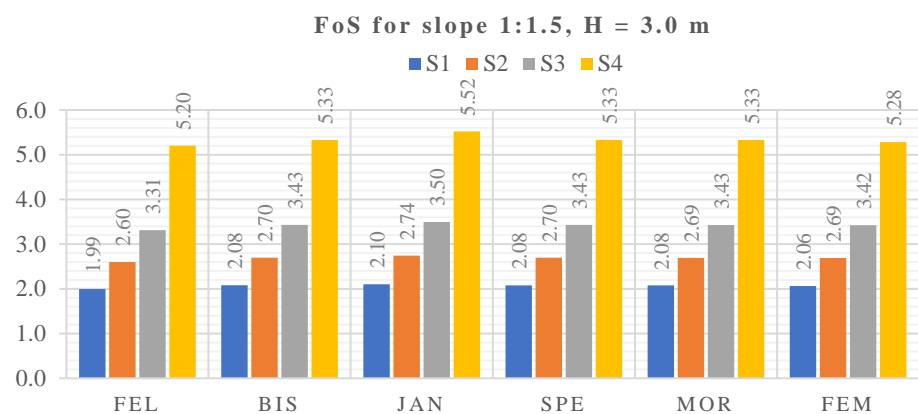|	Soil Type		S1				S2		
	Method	FoS	XC	YC	R	FoS	XC	YC	R
LEM (Slide)	Fellenius	1.994	1.600	4.296	4.711	2.602	1.646	4.357	4.741
	Bishop simplified	2.081	1.508	5.210	5.432	2.698	1.600	4.966	5.216
	Janbu corrected	2.102	1.554	4.783	5.094	2.743	1.646	4.783	5.062
	Spencer	2.079	1.508	5.210	5.432	2.696	1.600	4.905	5.170
	Morgenstern–Price	2.077	1.508	5.210	5.432	2.695	1.600	4.905	5.170
FEM (Plaxis)—circular		2.063	1.374	5.626	5.919	2.689	1.558	5.598	6.048
	Soil Type		S3				S4		
	Method	FoS	XC	YC	R	FoS	XC	YC	R
LEM (Slide)	Fellenius	3.314	1.692	4.357	4.726	5.203	1.866	4.513	6.110
	Bishop simplified	3.431	1.646	4.783	5.062	5.329	1.720	4.513	4.834
	Janbu corrected	3.495	1.646	4.783	5.062	5.521	1.866	5.123	6.539
	Spencer	3.429	1.646	4.783	5.062	5.330	1.720	4.513	4.834
	Morgenstern–Price	3.427	1.646	4.783	5.062	5.328	1.720	4.513	4.834
FEM (Plaxis)—circular		3.423	1.564	5.366	5.908	5.282	1.986	5.417	6.793

Figure 16. FoS for Slope 1:1.5, H = 3.00 m, S1–S4.

Table 4. Results for slope 1:1.5, H = 8.0 m, S1 = S4.

Soil Type		S1				S2			
	Method	FoS	XC	YC	R	FoS	XC	YC	R
LEM (Slide)	Fellenius	1.170	2.270	13.973	14.159	1.464	2.710	13.364	13.638
	Bishop simplified	1.224	1.390	15.040	15.104	1.532	1.976	14.354	14.490
	Janbu corrected	1.223	1.976	14.354	14.490	1.532	2.563	13.592	13.830
	Spencer	1.222	1.390	15.040	15.104	1.528	1.976	14.354	14.490
	Morgenstern–Price	1.221	1.390	15.040	15.104	1.528	1.976	14.354	14.490
	FEM (Plaxis)	1.195	1.161	17.484	17.706	1.509	1.859	16.742	17.024
Soil Type		S3				S4			
	Method	FoS	XC	YC	R	FoS	XC	YC	R
LEM (Slide)	Fellenius	1.844	2.930	13.059	13.381	2.513	3.957	11.230	11.912
	Bishop simplified	1.930	2.050	14.278	14.422	2.601	3.737	11.687	12.270
	Janbu corrected	1.931	2.563	13.592	13.830	2.655	3.664	11.840	12.390
	Spencer	1.925	2.050	14.278	14.422	2.599	3.590	11.992	12.510
	Morgenstern–Price	1.925	2.050	14.278	14.422	2.597	3.737	11.687	12.270
	FEM (Plaxis)	1.844	2.930	13.059	13.381	2.604	3.915	14.845	15.915
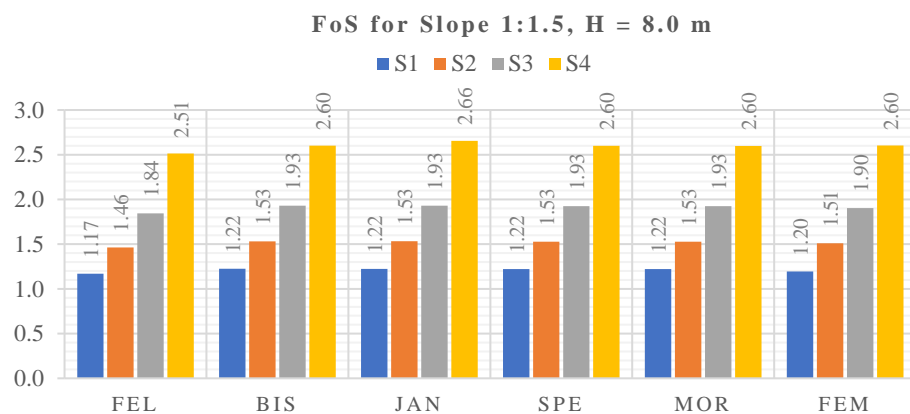
Figure 17. FoS for Slope 1:1.5, H = 8.00 m, S1–S4.

Table 5. Results for slope 1:1, H = 3.0 m.

Soil Type		S1				S2			
	Method	FoS	XC	YC	R	FoS	XC	YC	R
LEM (Slide)	Fellenius	1.752	0.565	4.864	4.897	2.298	0.703	4.620	4.674
	Bishop simplified	1.785	0.382	5.169	5.183	2.338	0.382	5.169	5.183
	Janbu corrected	1.851	0.382	5.169	5.183	2.440	0.382	5.169	5.183
	Spencer	1.784	0.382	5.169	5.183	2.338	0.382	5.169	5.183
	Morgenstern–Price	1.784	0.382	5.169	5.183	2.337	0.382	5.169	5.183
	FEM (Plaxis)	1.678	0.113	5.237	5.260	2.210	0.283	5.183	5.225
Soil Type		S3				S4			
	Method	FoS	XC	YC	R	FoS	XC	YC	R

Table 5. *Cont.*

	Soil Type		S1				S2		
	Method	**FoS**	**XC**	**YC**	**R**	**FoS**	**XC**	**YC**	**R**
LEM (Slide)	Fellenius	2.931	0.703	4.620	4.674	4.707	0.978	4.071	4.190
	Bishop simplified	2.980	0.565	4.864	4.897	4.738	0.978	4.071	4.190
	Janbu corrected	3.116	0.382	5.169	5.183	5.106	0.565	4.864	4.897
	Spencer	2.980	0.565	4.864	4.897	4.878	0.290	5.291	5.306
	Morgenstern–Price	2.978	0.565	4.864	4.897	4.794	0.428	5.108	5.121
	FEM (Plaxis)	2.821	0.334	5.159	5.195	4.489	0.782	5.210	5.325

Figure 18. FoS for Slope 1:1, H = 3.00 m, S1–S4.

Table 6. Results for slope 1:1, H = 8.0 m.

	Soil Type		S1				S2		
	Method	**FoS**	**XC**	**YC**	**R**	**FoS**	**XC**	**YC**	**R**
LEM (Slide)	Fellenius	0.962	−0.754	12.235	12.255	1.222	−0.020	11.778	11.771
	Bishop simplified	0.994	−1.047	12.388	12.431	1.258	−0.387	12.007	12.011
	Janbu corrected	1.011	−0.901	12.311	12.343	1.287	−0.387	12.007	12.011
	Spencer	0.992	−1.047	12.388	12.431	1.256	−0.387	12.007	12.011
	Morgenstern−Price	0.992	−0.974	12.388	12.413	1.255	−0.460	12.083	12.081
	FEM (Plaxis)	0.947	−2.204	15.199	15.376	1.190	−1.716	14.472	14.705
	Soil Type		S3				S4		
	Method	FoS	XC	YC	R	FoS	XC	YC	R
LEM (Slide)	Fellenius	1.545	−0.020	11.778	11.771	2.193	1.464	10.518	11.016
	Bishop simplified	1.589	−0.387	12.007	12.011	2.227	0.950	10.975	11.016
	Janbu corrected	1.630	−0.387	12.007	12.011	2.353	0.143	14.785	14.786
	Spencer	1.588	−0.387	12.007	12.011	2.222	1.317	10.670	10.736
	Morgenstern−Price	1.586	−0.387	12.007	12.011	2.227	0.950	10.975	11.016
	FEM (Plaxis)	1.501	−1.315	13.789	13.944	2.130	0.032	14.438	14.537
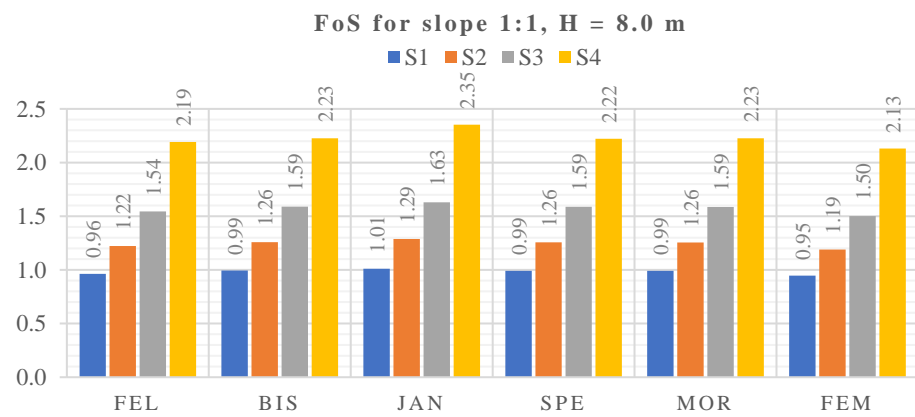
Figure 19. FoS for Slope 1:1, H = 8.00 m, S1–S4.

Table 7. Results for slope 2:1, H = 3.0 m.

	Soil Type	S1				S2			
	Method	FoS	XC	YC	R	FoS	XC	YC	R
LEM (Slide)	Fellenius	1.405	−1.350	4.681	4.866	1.869	−1.029	4.437	4.554
	Bishop simplified	1.396	−1.350	4.681	4.866	1.853	−1.029	4.437	4.554
	Janbu corrected	1.512	−1.625	4.864	5.122	2.034	−1.533	4.803	5.036
	Spencer	1.639	−2.166	7.790	7.873	2.203	−0.799	7.729	7.768
	Morgenstern−Price	1.631	−1.212	7.790	7.881	2.186	0.576	2.365	2.672
FEM (Plaxis)		1.389	−1.473	5.429	5.666	1.860	−1.267	5.293	5.481
	Soil Type	S3				S4			
	Method	FoS	XC	YC	R	FoS	XC	YC	R
LEM (Slide)	Fellenius	2.392	−1.029	4.437	4.554	3.985	−0.799	4.254	4.328
	Bishop simplified	2.371	−1.029	4.437	4.554	3.941	−0.249	3.767	3.772
	Janbu corrected	2.610	−1.441	4.742	4.951	4.421	−1.808	7.851	8.052
	Spencer	2.812	0.668	2.243	2.565	4.752	−0.020	7.546	7.549
	Morgenstern−Price	2.790	0.622	2.304	2.618	4.635	0.255	1.938	2.702
FEM (Plaxis)		2.379	−1.268	5.424	5.612	3.970	−0.535	4.955	5.106
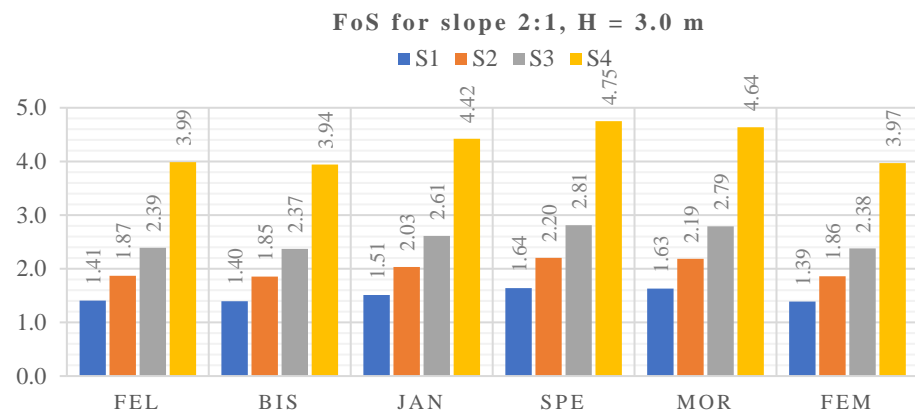
Figure 20. FoS for Slope 2:1, H = 3.00 m, S1–S4.

Table 8. Results for slope 2:1, H = 8.0 m.

| Soil Type		S1				S2			
	Method	FoS	XC	YC	R	FoS	XC	YC	R
LEM (Slide)	Fellenius	0.745	−4.059	10.172	10.951	0.961	−3.619	10.324	10.934
	Bishop simplified	0.741	−2.959	8.724	9.211	0.951	−2.812	8.724	9.160
	Janbu corrected	0.792	−4.573	11.544	12.404	1.022	−4.426	11.620	12.433
	Spencer	0.762	−4.206	11.848	12.544	1.007	−3.106	12.382	12.759
	Morgenstern−Price	0.766	−3.986	11.925	12.565	1.009	−3.106	12.458	12.806
	FEM (Plaxis)	0.598	−7.835	17.389	19.126	0.886	−7.202	16.031	17.663
Soil Type		S3				S4			
	Method	FoS	XC	YC	R	FoS	XC	YC	R
LEM (Slide)	Fellenius	1.219	−4.426	11.620	12.433	1.803	−1.749	10.461	10.605
	Bishop simplified	1.206	−2.739	8.724	9.134	1.762	−1.162	8.327	8.407
	Janbu corrected	1.299	−4.426	11.620	12.433	1.956	−2.996	12.442	12.788
	Spencer	1.290	−2.812	12.534	12.833	2.038	0.085	13.509	13.504
	Morgenstern−Price	1.285	−2.886	12.534	12.838	2.015	−0.135	13.509	13.487
	FEM (Plaxis)	1.171	−7.384	15.778	17.502	1.786	−3.974	14.841	15.487
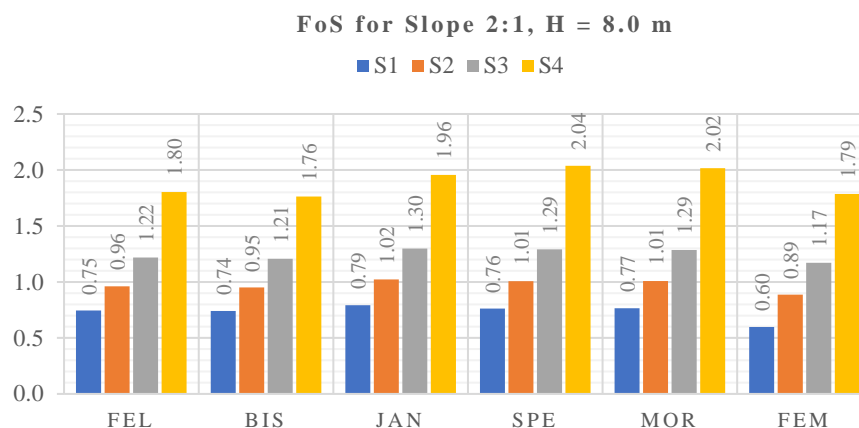
Figure 21. FoS for Slope 2:1, H = 8.00 m, S1–S4.

Knowledge of the critical slip surface profile beneath the landslide is essential for stability analysis and design of remedial works. Hence, the study selected different models for the slip surface and utilized the measurements of displacements performed in FEM to forecast the position and shape of the slip surface, accepting that this surface is not necessarily circular.

By observation, the study selected three distinct models for the potential slip surface, i.e., a damped sinusoid, a second-degree parabola, and a logarithmic spiral determined by both polar and Cartesian coordinates, by using the same picked-up points as for the circular slip surfaces already defined in each case investigated, which were considered benchmarks for these models.

Figure 22 shows a log-spiral failure curve and the associated parameters used in the current characterization. Functions $Y_s(x)$ and $Y_f(x)$ describe slope surface and failure surface, respectively. $Y_f(x)$ corresponds to a log spiral, described by 'r' in polar coordinates. Coordinates (X_c, Y_c) represent the pole of the log spiral of the Cartesian system with the origin at the toe of the slope. That is the reason why (X_s, Y_s) and (X_e, Y_e) are the coordinates at which the failure surface intersects the slope surface, associated with angles θ_s and θ_e of

polar coordinates [33]. The log-spiral failure surface predicts the critical failure surface of different 2D slope geometries studied using an optimization process.
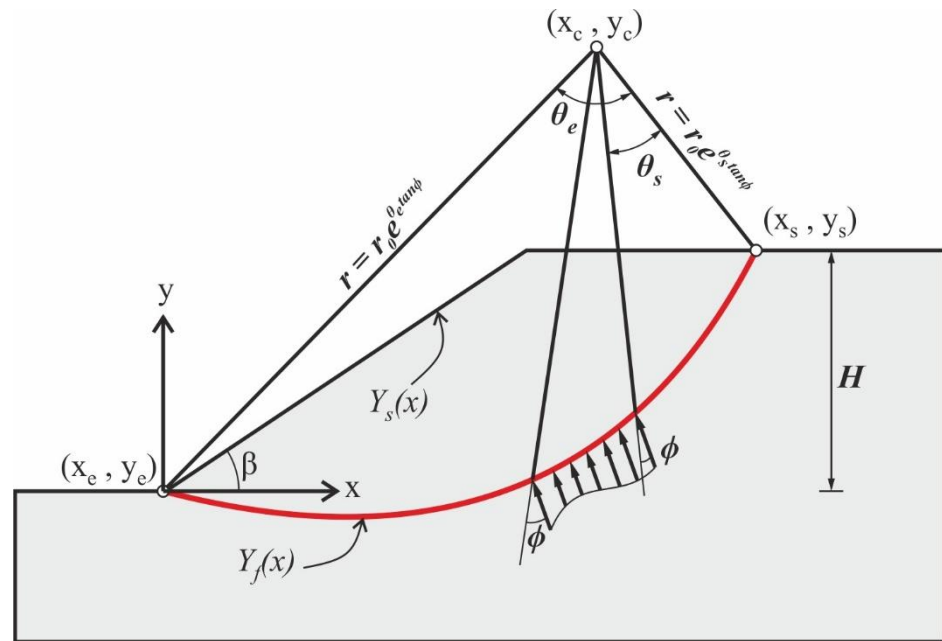

Figure 22. The log-spiral failure surface (after [33]).

The equations corresponding to the three types of slip surface models are the following:

$$\text{Damped sinusoid}: \qquad y = A \cdot e^{-\gamma t} \cdot \cos(\omega t + \phi) - B \qquad (3)$$

$$\text{Second} - \text{degree parabola}: \quad y = A \cdot x^2 + B \cdot x + C \qquad (4)$$

$$\text{Logarithmic} - \text{spiral 1}: \qquad r = r_o e^{\theta tg\varphi} \text{ (polar coordinates)} \qquad (5)$$

where r is the spiral radius (i.e., distance from the pole to the failure surface), r_o is the radius value for = 0°, and ϕ is the friction angle of the material.

$$\text{Logarithmic spiral 2}: \qquad y(t) = ae^{bt}\sin(t) \text{ (Cartesian coordinates)} \qquad (6)$$

The most efficient approach for finding coefficients that minimize the error for these models was also to use least-squares optimization. Table 9 presents the fitting parameters for the damped sinusoid and second-degree parabola for all cases considered, necessary to plot a potential critical slip surface as close as possible to that determined by the picked-up points.

Table 9. Fitting parameters for the damped sinusoid and second-degree parabola for all the considered cases.

Slope	Hight	Soil Type	Damped Sinusoid $y = A \cdot e^{-\gamma t} \cdot \cos(\omega t + \phi) - B$					Second−Degree Parabola $y = A \cdot x^2 + B \cdot x + C$		
			A	ω	φ	γ	B	A	B	C
1:1.5	3.0 m	S1	50.024	0.052	3.849	−0.052	−37.952	0.124	−0.402	−0.044
		S2	57.596	0.054	3.633	−0.036	−50.601	0.121	−0.426	−0.162
		S3	60.563	0.056	3.535	−0.030	−55.660	0.123	−0.427	−0.280
		S4	74.381	0.054	2.939	0.005	−71.736	0.104	−0.422	−1.108
	8.0 m	S1	77.753	0.032	3.220	−0.005	−77.576	0.043	−0.219	0.062
		S2	63.134	0.029	3.683	−0.021	−54.063	0.044	−0.268	0.067

Table 9. *Cont.*

Slope	Hight	Soil Type	Damped Sinusoid $y = A{\cdot}e^{-\gamma t}{\cdot}\cos(\omega t+\phi)-B$					Second$-$Degree Parabola $y = A{\cdot}x^2+B{\cdot}x+C$		
			A	ω	ϕ	γ	B	A	B	C
		S3	62.264	−0.038	3.769	0.020	−49.316	0.036	−0.275	−1.140
		S4	32.854	−0.044	2.866	−0.023	−31.173	0.047	−0.434	−0.342
1:1	3.0 m	S1	3.572	0.000	4.765	−0.583	0.260	0.161	−0.219	0.062
		S2	8.327	0.016	4.689	−0.360	−0.126	0.157	−0.243	0.044
		S3	1.699	0.000	4.798	−0.613	0.229	0.159	−0.262	0.063
		S4	11.259	0.033	4.557	−0.238	−1.664	0.145	−0.322	0.018
	8.0 m	S1	65.402	0.037	3.673	−0.021	−56.557	0.063	−0.057	0.213
		S2	65.545	0.037	3.665	−0.021	−56.799	0.063	−0.066	0.052
		S3	66.168	0.039	3.637	−0.022	−58.359	0.070	−0.142	0.190
		S4	4.203	0.000	4.852	−0.207	0.825	0.059	−0.201	0.170
2:1	3.0 m	S1	3.016	−0.019	4.894	−0.648	0.603	0.195	0.075	0.014
		S2	2.378	−0.023	4.877	−0.772	0.433	0.201	0.016	0.038
		S3	3.110	−0.017	4.873	−0.650	0.568	0.193	0.030	0.020
		S4	0.993	−0.021	4.826	−1.134	0.212	0.193	−0.120	−0.039
	8.0 m	S1	7.766	−0.012	4.876	−0.337	1.182	0.067	0.291	0.081
		S2	9.021	−0.009	4.833	−0.368	1.026	0.077	0.250	0.075
		S3	8.493	−0.010	4.840	−0.381	0.080	0.267	0.073	0.080
		S4	9.082	−0.005	4.783	−0.378	0.639	0.072	0.052	0.090

Then, the study found the fitting parameters for the log spiral using the same optimization method, with slight differences in the results achieved in polar coordinates compared to those obtained in the Cartesian system in all cases. Then, the study compared the values of the fitting errors for each type of slip surface investigated with the fitting errors of the classical circular benchmark slip surface calculated above (Table 10).

Table 10. Fitting errors of regression curves for five distinct shapes of the potential slip surface (the circular benchmark slip surface included) and three distinct slope gradients for the discussed cases.

Slope	Hight	Soil Type	Fitting Shape				
			Shape 1	Shape 2	Shape 3	Shape 4	Shape 5
1:1.5	3.0 m	S1	0.438	0.057	0.104	0.069	0.162
		S2	0.860	0.109	0.147	0.092	0.307
		S3	1.273	0.132	0.149	0.108	0.296
		S4	7.541	0.460	0.465	0.471	1.014
	8.0 m	S1	0.573	0.480	0.527	0.082	0.263
		S2	0.792	0.272	0.682	0.136	0.445
		S3	9.166	0.808	1.752	1.238	1.828
		S4	4.831	0.745	1.140	0.544	1.638
1:1	3.0 m	S1	0.143	0.182	0.358	0.128	0.117
		S2	0.106	0.161	0.331	0.093	0.088
		S3	0.097	0.136	0.362	0.077	0.085
		S4	0.087	0.172	0.340	0.077	0.068
	8.0 m	S1	0.389	0.230	0.379	1.504	0.345
		S2	0.895	1.489	1.704	0.662	0.926
		S3	0.696	1.276	1.354	0.363	0.538
		S4	1.750	2.132	3.572	1.438	1.781

Table 10. *Cont.*

Slope	Hight	Soil Type	Fitting Shape				
			Shape 1	Shape 2	Shape 3	Shape 4	Shape 5
2:1	3.0 m	S1	0.139	0.054	0.028	0.135	0.057
		S2	0.057	0.016	0.020	0.041	0.029
		S3	0.208	0.095	0.041	0.130	0.101
		S4	0.536	0.042	0.053	0.081	0.152
	8.0 m	S1	0.673	0.069	0.187	0.594	2.232
		S2	1.036	0.061	0.207	0.234	0.626
		S3	1.237	0.037	0.183	0.206	0.764
		S4	1.537	0.114	0.341	0.887	0.779

Shape 1—circle, Shape 2—damped sinusoid, Shape 3—second-degree parabola, Shape 4—log-spiral 1 (polar coordinates), Shape 5—log-spiral 2 (Cartesian coordinates).

Figure 23a–c shows the graphs of the regression curves for five distinct shapes of the potential slip surface, including the benchmark (the circular slip surface) for three different slope gradients and H = 3, S1.
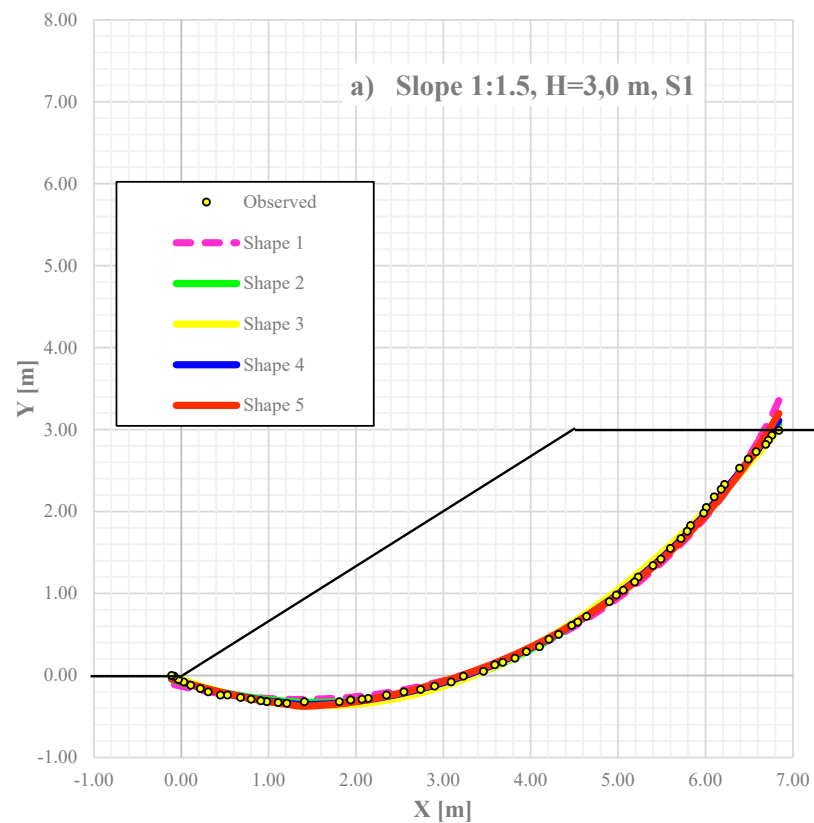
Figure 23. *Cont.*
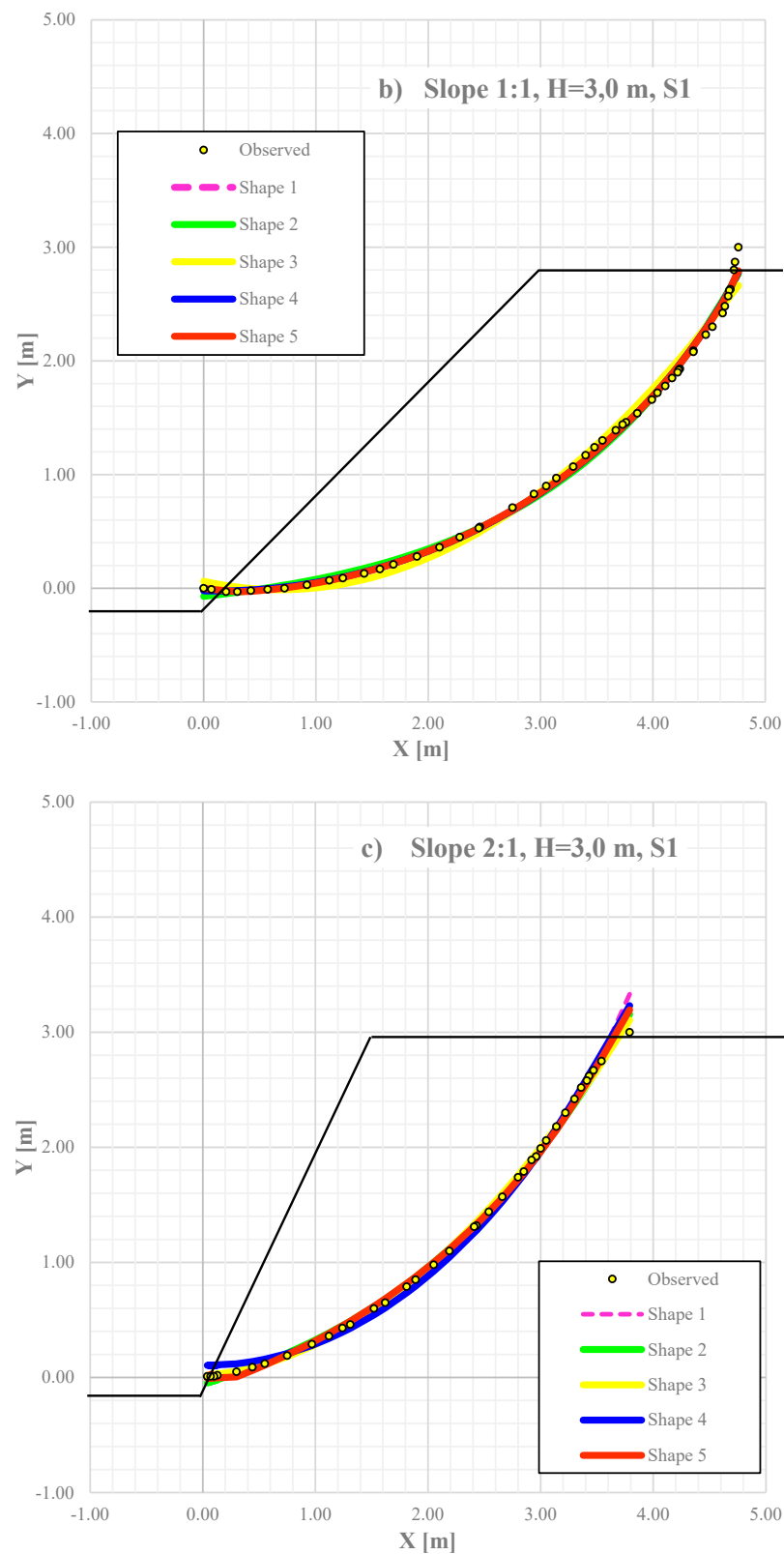
Figure 23. Graphs of regression curves for five distinct shapes of the potential slip surface and three distinct slope gradients, H = 3, S1.

The results in Figure 23 show that, as expected, the logarithmic spiral seems to fit best for 1:1.5 and 1:1 slopes, while, unexpectedly, the optimal shape for 2:1 steep slopes

is a damped sinusoid. However, the parabola seems to verify some cases quite well. The circular surface does not seem to confirm any case taken into account.

4. Discussion and Conclusions

This study proposes a sustainable slope stability analysis by comparing distinct methods. The goal of the study was to obtain valuable information on the factor of safety and render evidence on failure mechanisms through critical slip surface determination. Examples of slope stability analysis were performed on homogenous slopes with three distinct slope gradients (1:1.5; 1:1; 2:1), two definite slope heights (H-3 m; H-8 m), and four different soil characteristics (S1–S4) from non-plastic clayey sands to cohesive clays. In terms of types of soils, i.e., S1—clayey silt, S2—sandy-clayey silt, S3—sandy-silty clay, and S4—clay, they were selected due to their distinct mechanical characteristics to model different types of soil shear strengths. Based on the findings, the following statements are conclusive:

- The stability analysis compared the safety factor values obtained by the limit equilibrium method with those resulting from the upper-bound analysis by connecting the advantages provided by the upper-bound theorem with the finite element method through a strength reduction method with displacement-based finite element method (strength reduction finite element analysis).
- Numerical models run in PLAXIS 2D using these data led to accurate results regarding the factor of safety compared to those obtained in Slope2 Rocscience using five LE methods (Fellenius, Bishop simplified, Janbu corrected, Spencer, and Morgenstein–Price). The comparison has significant importance for verifying slope stability requirements.
- The results being in good agreement in the cases taken into account show the influence of the slope geometry on the safety factor. Varying the slope angle gradually while keeping the height of the slope constant, the factor of safety increases as the slope angle decreases for the same type of soil, as Tables 3–8 show. The decrease in slope increases the factor of safety almost linearly. There is a strong and opposite relation between slope angle and factor of safety for the four types of soils. Results also show that the FoS (stability, implicitly) is dependent of the slope height, even in the case of homogeneous slopes. The factor of safety increases as the slope height decreases, as the pair of Tables 3–8 show for the same type of soil and gradient. Additionally, at a lower height, i.e., 3 m, the failure mode in clays (S4) tends to be base slide for all the three gradients, while at 8 m height, the failure mode tends to be toe slide. All these results indicate a strong relationship between the slope height and the factor of safety. In this regard, the geometry of the slope (height and angle) may and should be optimized to maximize the slope factor of safety.
- The mesh shape has a limited influence on the slope stability in FEM. However, both mesh size and density significantly influence the shape of the slip surface. Hence, the study adopted a local mesh refinement in the critical area and sparse mesh in the other areas. Furthermore, the adaptive mesh refinement influences the error margins.
- Even though the comparison of the factor of safety resulting from the analysed methods shows a slight difference, this approach indicates a fundamental difference in their basic principles. While the LE method relies on the formulations of the limit equilibrium dependent on a static force or moment equilibrium, the other formulation depends on the stress–strain relationship. It finds a critical slip surface where the excessive strains are localised and computes the FoS by a c-phi reduction procedure for the Mohr–Coulomb model. This analysis calculates the safety factor for each element along with the CSS. That makes the FoS more reliable than in the LE methods.
- Compared to LEM, numerical analysis does not require any a priori definition of the failure mechanism and provides accurate upper bounds of the (FoS) but is limited by the associated flow rules.
- Even though both methods provide tight values for safety factor estimation, potential slip surface, and the presumed centre of the slip surface, they have their advantages

and limitations. The values achieved indicate that the frequency of using the upper-bound limit method may be similar to using LEM in routine analysis and design, considering the limitations of each method in evaluating the results.

- Graphs of the regression curves for five distinct shapes of the critical slip surface, including the benchmark (the circular slip surface), show that the shape of the slip surface is not necessarily the same in the case of the same slope example. Depending on the slope geometry and material, a critical slip surface may develop layouts closer to a logarithmic spiral, damped sinusoid, parabola, or circle. Presented results could serve as a starting point for further research on the shape of the CSS. They should further progress to provide relevant interpretations summarized in the form of regression curves for some other shapes, defining the most probable shape of the CSS using various equations.

- The conclusion from the above discussion states that reliable methods are available for searching for critical slip surfaces and calculating the safety factor for a slope. However, no approach can involve all the uncertainties that emerged in the safety factor and CSS calculus, on the one hand, and the shape of the CSS still needs to be attentively studied, on the other hand. Thus, slope stability analysis requires an increasingly accurate strategy.

For non-homogeneous slopes, because of the material interruption at the interface, the discontinuity of the slope material parameters inevitably leads to discontinuities of the stress field occurring along the interfaces of each layer. That brings difficulties to the direct use of a classical optimization algorithm for CSS search. For this reason, the sliding surface search can rely on the global procedure of slope stability, which takes the whole slip mass and does not introduce inter-slice forces, leading to a much smaller scale of computations compared to the method of slices. The non-linearity can be reduced by treating the safety factor as an independent variable like other variables. The material interruption in c and φ of a non-homogeneous slope should be expressed by a function to achieve continuous and smoothing internal material parameters. A series of discrete points in the potential slip surface can be set up, reaching convergence after a consistent iteration process and determining the FoS and the shape of the CSS. This study envisages a continuation of the research that takes into account the non-homogeneity of the slope.

References

1. Mansour, Z. Traditional Methods vs. Finite Difference Method for Computing Safety Factors of Slope Stability. *Electron. J. Geotech. Eng.* **2011**, *16*, 1119–1130.
2. Rezaei, A.; Hassani, H.; Moarefvand, P.; Golmohammadi, A. Determination of unstable tectonic zones in C–North deposit, Sangan, NE Iran using GPR method: Importance of structural geology. *J. Min. Environ. (JME)* **2019**, *10*, 177–195. [CrossRef]

3.   Fredlund, D.G. Analytical Methods for Slope Stability Analysis. In Proceedings of the Fourth International Symposium on Landslides, State-of-the-Art, Toronto, ON, Canada, 16–21 September 1984; pp. 229–250.

4.   Slide2 Slope Stability Verification Manual, Rocscience. Available online: https://static.rocscience.cloud/assets/verification-and-theory/Slide2/Slide_SlopeStabilityVerification.pdf (accessed on 18 March 2022).

5.   Fellenius, W. Calculation of the stability of earth dams. In *Transactions of the 2nd Congress on Large Dams*; International Commission on Large Dams (ICOLD): Washington, DC, USA; Paris, France, 1936; pp. 445–462.

6.   Salunkhe, D.P.; Chvan, G.; Bartakke, R.N.; Kothavale, P.R. An Overview on Methods for Slope Stability Analysis. *IJERT* **2017**, *6*, 528–535.

7.   Whitman, R.V.; Bailey, W.A. Use of computers for slope stability analysis. *J. Soil Mech. Found.* **1967**, *93*, 475–498. [CrossRef]

8.   Bishop, A.W. The use of slip circle in the stability analysis of earth slopes. *Geotechnique* **1955**, *5*, 7–17. [CrossRef]

9.   Janbu, N. Application of composite slip sufaces for stability analysis. In Proceedings of the European Conference on Stability of Earth Slopes 1954, Stockolm, Sweden, 1954; Volume 3, pp. 43–49.

10. Morgenstern, N.R.; Price, V.E. The analysis of the stability of general slip surfaces. *Geotechnique* **1965**, *15*, 79–93. [CrossRef]

11. Spencer, E. A method of analysis of the stability of embankments assuming parallel interslice forces. *Geotechnique* **1967**, *17*, 11–26. [CrossRef]

12. Memon, Y. A Comparison Between Limit Equilibrium and Finite Element Methods for Slope Stability Analysis. 2011. Available online: https://www.researchgate.net/publication/329697782_A_Comparison_Between_Limit_Equilibrium_and_Finite_Element_Methods_for_Slope_Stability_Analysis (accessed on 18 March 2022).

13. Ching, R.K.H.; Fredlund, D.D. Some difficulties associated with the limit equilibrium method of slices. *CGJ* **1983**, *20*, 662–672. [CrossRef]

14. Brunsden, D.; Prior, D.B. *Slope Instability (Landscape Systems)*; John Wiley & Sons: New York, NY, USA, 1984.

15. Morgenstern, N.R.; Price, V.E. A numerical method for solving the equations of stability of general slip surfaces. *Comput. J.* **1967**, *9*, 388–393. [CrossRef]

16. Kwo, O.L.A.; Guan, P.C.; Cheng, W.P.; Sun, C.T. Development of Meshfree Method for Slope Stability and Post-Failure Analyses. In Proceedings of the 2012 World Congress on Advances in Civil, Environmental, and Materials Research (ACEM' 12), Seoul, Korea, 26–30 August 2012.

17. Moudabel, O.A.M. Slope stability case study by limit equilibrium and numerical methods, @inproceedings{Moudabel2013SlopeSC}. 2013. Available online: https://www.semanticscholar.org/paper/Slope-stability-case-study-by-limit-equilibrium-and-Moudabel/4120125742f3d4f8e6f5fe4ac8385da9cbf2a827 (accessed on 18 March 2022).

18. Duncan, J.M. State of the art: Limit equilibrium and finite-element analysis of slopes. *JoGE* **1996**, *122*, 577–596. [CrossRef]

19. Ahmadabadi, M.; Ghanbari, A. New procedure for active earth pressure calculation in retaining walls with reinforced cohesive-frictional backfill. *Geotext. Geomembr.* **2009**, *27*, 456–463. [CrossRef]

20. Michalowski, R.L.; Zhao, A. Continuum versus structural approach to stability of reinforced soil. *J. Geotech. Eng.* **1995**, *121*, 152–162. [CrossRef]

21. Qin, C.B.; Chian, S.C. Kinematic analysis of seismic slope stability with a discretisation technique and pseudo-dynamic approach: A new perspective. *Géotechnique* **2017**, *68*, 492–503. [CrossRef]

22. Thomson, R.J. The location of critical slip surfaces in slope-stability problems. *J. S. Afr. Inst. Min. Metall.* **1993**, *93*, 85–95.

23. Li, E.; Zhuang, X.; Zheng, W.; Cai, Y. Effect of graph generation on slope stability analysis based on graph theory. *J. Rock Mech. Geotech. Eng.* **2014**, *6*, 380–386. [CrossRef]

24. Steward, T.; Sivakugan, N.; Shukla, S.K.; Das, B.M. Taylor's Slope Stability Charts Revisited. *IJOG* **2011**, *11*, 348–352. [CrossRef]

25. Alex, J.; Ammu, A.T.; Aparna, G.N.; Arshiq, M.P. Slope stability analysis using PLAXIS 2D. *IRJET* **2018**, *5*, 3666–3668.

26. Chehade, H.A.; Dias, D.; Sadek, M.; Jenck, O.; Chehade, F.H. Upper bound seismic limit analysis of geosynthetic-reinforced unsaturated soil walls. *Geotext. Geomembr.* **2020**, *48*, 419–430. [CrossRef]

27. Plaxis bv, Bentley Systems, Incorporated, Plaxis Connect Edition V22.00–General Information Manual. Available online: https://communities.bentley.com/cfs-file/__key/communityserver-wikis-components-files/00-00-00-05-58/PLAXIS2D_2D00_CE_2D00_V22.00_2D00_0_2D00_Gen_2D00_Info.pdf (accessed on 18 March 2022).

28. Sarma, S.K.; Tan, D. Determination of critical slip surface in slope analysis. *Geotechnique* **2006**, *56*, 539–550. [CrossRef]

29. Petterson, K.E. The Early History of Circular Sliding Surfaces. In *Géotechnique*; ICE Publishing: London, UK, 1955; Volume 5, pp. 275–296.

30. Petterson, K.E. The quay slide in Gothenburg on 5th March 1916. *Teknisk Tidskrift V.o.V.* **1916**, *46*, 471–478.

31. Petterson, K.E. A special foundation method for a structure in Gothenburg harbour. *Teknisk Tidskrift V.o.V.* **1941**, *71*, 45–52.

32. Fellenius, W. *Earth Static Calculations with Friction and Cohesion (Adhesion) and Assuming Circular Cylindrical Sliding Surfaces*; Swedish original 1926; Verlag Ernst & Sohn: Berlin, Germany, 1927.

33. Klar, A.; Aharonov, E.; Kalderon-Asael, B.; Katz, O. Analytical and observational relations between landslide volume and surface area. *J. Geophys. Res. Atmos.* **2011**, *116*, 10. [CrossRef]

34. Cao, J. Neural Network and Analytical Modeling of Slope Stability. Ph.D. Thesis, University of Oklahoma, Norman, OK, USA, 2002.

35. Niu, W. Determination of Slope Safety Factor with Analytical Solution and Searching Critical Slip Surface with Genetic-Traversal Random Method. *Sci. World J.* **2014**, *2014*, 950531. [CrossRef] [PubMed]

36. Repadi, J.A.; Bari, F.; Ismail, F.A.; Andriani, A.; Hakam, A. A new slip surface in noncohesive slopes. In Proceedings of the International Conference on Science in Engineering and Technology, Palu, Indonesia, 21–22 October 2020.

37. Fernandes, M.M. *Analysis and Design of Geotechnical Structures*; CRC Press (Taylor & Francis Group): Boca Raton, FL, USA, 2021.

38. Zhou, J.; Qin, C. Finite-element upper-bound analysis of seismic slope stability considering pseudo-dynamic approach. *Comput. Geotech.* **2020**, *122*, 103530. [CrossRef]

39. Oberhollenzer, S.; Tschuchnigg, F.; Schweiger, H.F. Finite element analyses of slope stability problems using non-associated plasticity. *J. Rock Mech. Geotech. Eng.* **2018**, *10*, 1091–1101. [CrossRef]

40. Li, S.H.; Luo, X.H.; Wu, L.Z. An improved whale optimization algorithm for locating critical slip surface of slopes. *Adv. Eng. Softw.* **2021**, *157–158*, 103009. [CrossRef]

41. Shiferaw, H.M. Study on the influence of slope height and angle on the factor of safety and shape of failure of slopes based on strength reduction method of analysis. *Beni-Suef Univ. J. Basic Appl. Sci.* **2021**, *31*, 10. [CrossRef]

42. Firomsa, W.; Tsige, D. Developing Model for Critical Slip Surface in Slope Stability Analysis based on Geometry and Soil parameters. *Saudi J. Civ. Eng.* **2021**, *5*, 60–73. [CrossRef]

43. Li, S.H.; Wu, L.Z.; Luo, X.H. A novel method for locating the critical slip surface of a soil slope. *Eng. Appl. Artif. Intell.* **2020**, *94*, 103733. [CrossRef]